NASA TECHNICAL MEMORANDUM

NASA TM X-53953

A SIMPLIFIED DEAD RECKONING NAVIGATION SYSTEM FOR THE MANNED LUNAR ROVING VEHICLE

By Walter L. Green
Astrionics Laboratory

September 30, 1969

NASA

George C. Marshall Space Flight Center
Marshall Space Flight Center, Alabama

MSFC - Form 3190 (September 1968)

TECHNICAL REPORT STANDARD TITLE PAGE

1. REPORT NO.	2. GOVERNMENT ACCESSION NO.	3. RECIPIENT'S CATALOG NO.
TM X-53953		

4. TITLE AND SUBTITLE	5. REPORT DATE
A Simplified Dead Reckoning Navigation System for the Manned Lunar Roving Vehicle	September 30, 1969
	6. PERFORMING ORGANIZATION CODE
7. AUTHOR(S) Walter L. Green	8. PERFORMING ORGANIZATION REPORT #
9. PERFORMING ORGANIZATION NAME AND ADDRESS George C. Marshall Space Flight Center Marshall Space Flight Center, Alabama 35812	10. WORK UNIT NO.
	11. CONTRACT OR GRANT NO.
12. SPONSORING AGENCY NAME AND ADDRESS	13. TYPE OF REPORT & PERIOD COVERED Technical Memorandum
	14. SPONSORING AGENCY CODE

15. SUPPLEMENTARY NOTES

Prepared by: Astrionics Laboratory
Science and Engineering Directorate

16. ABSTRACT

A dead reckoning navigation system for the manned lunar roving vehicle is presented. The basic hardware for the system is two free gyros mounted to the frame of the vehicle, the wheel odometers and tachometers, and a signal processor. The mathematical equations for the navigation system are developed and related directly to the vehicle velocity and the gimbal angle readings. A digital simulation program is written for the navigation system for performing error analysis. The simulation can be used for determining the effects of gyro drifts and system misalignments for any selected lunar surface profile. The results of a study with selected ranges of gyro drift rates and misalignments for a particular surface profile are given.

17. KEY WORDS	18. DISTRIBUTION STATEMENT
Dead reckoning navigation Lunar roving vehicle	Announce in STAR See Document Release Form

19. SECURITY CLASSIF. (of this report)	20. SECURITY CLASSIF. (of this page)	21. NO. OF PAGES	22. PRICE
Unclassified	Unclassified	66	$3.00

MSFC - Form 3292 (May 1969)

ACKNOWLEDGMENTS

This work was suggested as a summer work assignment by Mr. Nikolaus Neudatschin of the Astrionics Laboratory, MSFC. Mr. Neudatschin made several helpful suggestions during the course of the project. The author is also grateful to Mr. Ken Fernandez who wrote the simulation program and provided the computer results.

TABLE OF CONTENTS

LIST OF ILLUSTRATIONS

LIST OF ILLUSTRATIONS (Continued)

LIST OF ILLUSTRATIONS (Concluded)

TECHNICAL MEMORANDUM X-53953

A SIMPLIFIED DEAD RECKONING NAVIGATION SYSTEM FOR THE MANNED LUNAR ROVING VEHICLE

INTRODUCTION

Problems related to lunar surface exploration have been studied by MSFC for the past several years. Early in these studies, a vehicle capable of navigating over the lunar surface was required. Subsequently, several industrial firms proposed and fabricated candidate lunar surface vehicles. In addition, analytical studies concerning lunar navigation and exploration have been carried out [1-6].

More recently, plans are being developed for exploration in the 1972-1980 time-frame. Current work is being directed to the development of two vehicles. The first one, used in early exploration, is the manned lunar roving vehicle (MLRV). This system will be driven by an astronaut onboard and will require dead reckoning navigation. The second system, used in advanced exploration, is the dual mode lunar roving vehicle (DMLRV). This system will be driven by either an astronaut onboard or by earth-controlled remote methods. In addition to dead reckoning navigation, a position-fix system will also be required on the DMLRV.

Many concepts for dead reckoning navigation have been proposed [5]. The navigation hardware for implementing these concepts includes various combinations of vertical gyros, directional gyros, pendulous inclinometers, accelerometers, sun sensors, star trackers, doppler radar, IR and rf earth trackers, and odometers.

This paper gives a technique for dead reckoning navigation of an MLRV. The hardware involved consists of two free gyros hard-mounted to the frame of the vehicle, odometers, and tachometers. For the system to be self-contained, some form of signal processing (small computer) will also be needed.

The salient requirements of the MLRV navigation system are:

1. Navigation within a 5-km radius of the lunar excursion module (LEM). Within the 5-km radius the lunar roving vehicle (LRV) will travel up to 30 km.

2. An indication of the total distance traveled, with an accuracy of ±2 percent, must be available.

3. At a 5-km radial distance, the heading to the LEM must be known within ±3 degrees.

4. The navigation system must be capable of returning the LRV within 500 meters of the LEM.

5. The system must have the capability of revisiting an established site. (Without visual cues this may be difficult to accomplish since an accuracy of better than 500 meters would be required.)

6. The LRV must be capable of sorties of a maximum 3-hour duration.

7. The LRV must be capable of a 3-day period of lunar exploration.

CHARACTERISTICS OF THE PROPOSED NAVIGATION SYSTEM

First it should be stated that there are many navigation schemes, with better accuracy than the one proposed, which will satisfy the above requirements. However, high resolution navigation systems carry with them the penalty of an increase in weight, volume, and complexity. The proposed two-free-gyro system is easy to implement and relatively light in weight.

The system is defined by the following characteristics. At time = 0 (the start of any given exploration trip), vehicle body axes and moon-fixed inertial axes are aligned with one another. This can be accomplished by caging the gyros and bringing the gyro rotors up to full speed while in the caged condition. The orientation of the coordinates is arbitrarily defined by the alignment of the vehicle with any outstanding landmark. It is desirable that this landmark be recognizable from local terrain photographs. The center of the coordinate systems is on the surface of the moon and in the general vicinity of the shelter (LEM) site. As the moon rotates around its polar axis, the origin of the moon-fixed inertial coordinate system also rotates with the surface

of the moon. The total velocity of the vehicle, relative to the surface of the moon, is resolved into components along the X, Y, and Z axes of the moon-fixed inertial system. These components are integrated to give the distance traveled relative to the moon coordinate system. For the system to be completely accurate the moon-fixed reference system should be Schuler-tuned to remain fixed relative to the moon's surface. However, during any 3-hour sortie the moon will rotate a maximum of approximately 1.5 degrees. Neglecting this rotation will introduce small errors in the reference bearing of the vehicle, the heading of the vehicle with respect to the shelter area, and the distance traveled relative to the moon reference system. As stated previously, Schuler tuning can be employed to eliminate these small errors, but the added complexity is not justified. The MLRV navigation requirements can be met using state-of-the-art gyros (with their associated drift rates) without Schuler tuning.

COORDINATE SYSTEM DEFINITION

Assume that the vehicle body coordinate system is defined so that the X axis is along the aft-forward sense with X positive in the forward direction. The Z axis is perpendicular to the X axis and positive upward. The Y axis completes a right-hand orthogonal coordinate system. This set of axes will be denoted by the subscript "B" to indicate body axes (X_B, Y_B, Z_B). A sketch of the coordinate system located in the vehicle frame is shown in Figure 1.

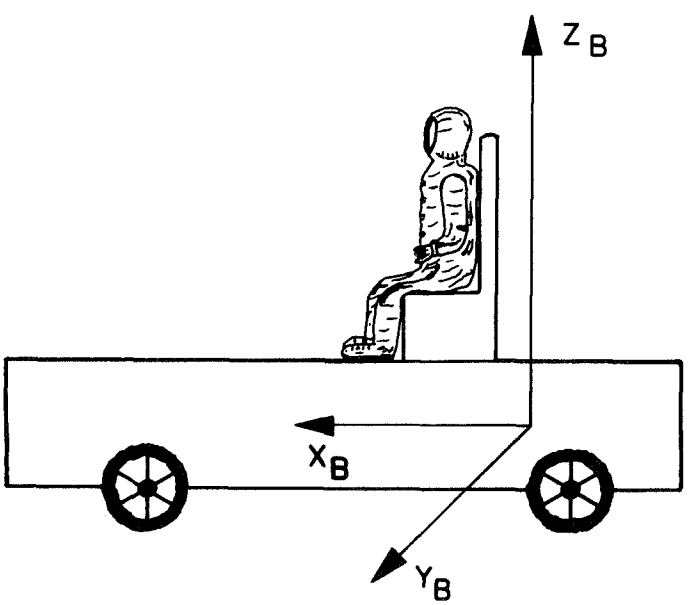

Figure 1. Vehicle body coordinate system.

An inertial coordinate system with its center at the LEM site and whose origin moves with the moon rotation is defined so that it is initially aligned to the body coordinates at $t = 0$. The coordinates of this system are given by X_I, Y_I, and Z_I.

At any time, the body coordinate system can be located with respect to the X_I, Y_I, Z_I system by a set of sequential rotations. Many such sets of rotations exist that can serve this purpose. However, by selecting the sequential rotations in a certain way, information can be obtained which will allow one to determine the body axes location (relative to the X_I, Y_I, Z_I frame) by direct readings of gimbal pickoffs from the gyros. A method for accomplishing this is given later.

In the work that follows, the mathematical equations for the navigation system are derived. The variables for these equations are related directly to the gimbal angles of the gyros. Thus knowledge of the vehicle velocity and the gimbal angles are sufficient for determining the vehicle position, bearing, and heading with respect to the shelter site.

DEVELOPMENT OF THE NAVIGATION SYSTEM EQUATIONS

Consider the schematic of two free gyros mounted to the vehicle frame as shown in Figure 2. Initially the X_B, Y_B, Z_B frame is aligned to the X_I, Y_I, Z_I frame. Four gimbal angles are defined on the diagram. Two transformations relating the X_B, Y_B, Z_B axes to the X_I, Y_I, Z_I axes are given as follows.

$$\begin{vmatrix} X \\ Y \\ Z \end{vmatrix}_B = [A2(Z)]\,[A1(Y)]\,[U(X)] \begin{vmatrix} X \\ Y \\ Z \end{vmatrix}_I , \qquad (1)$$

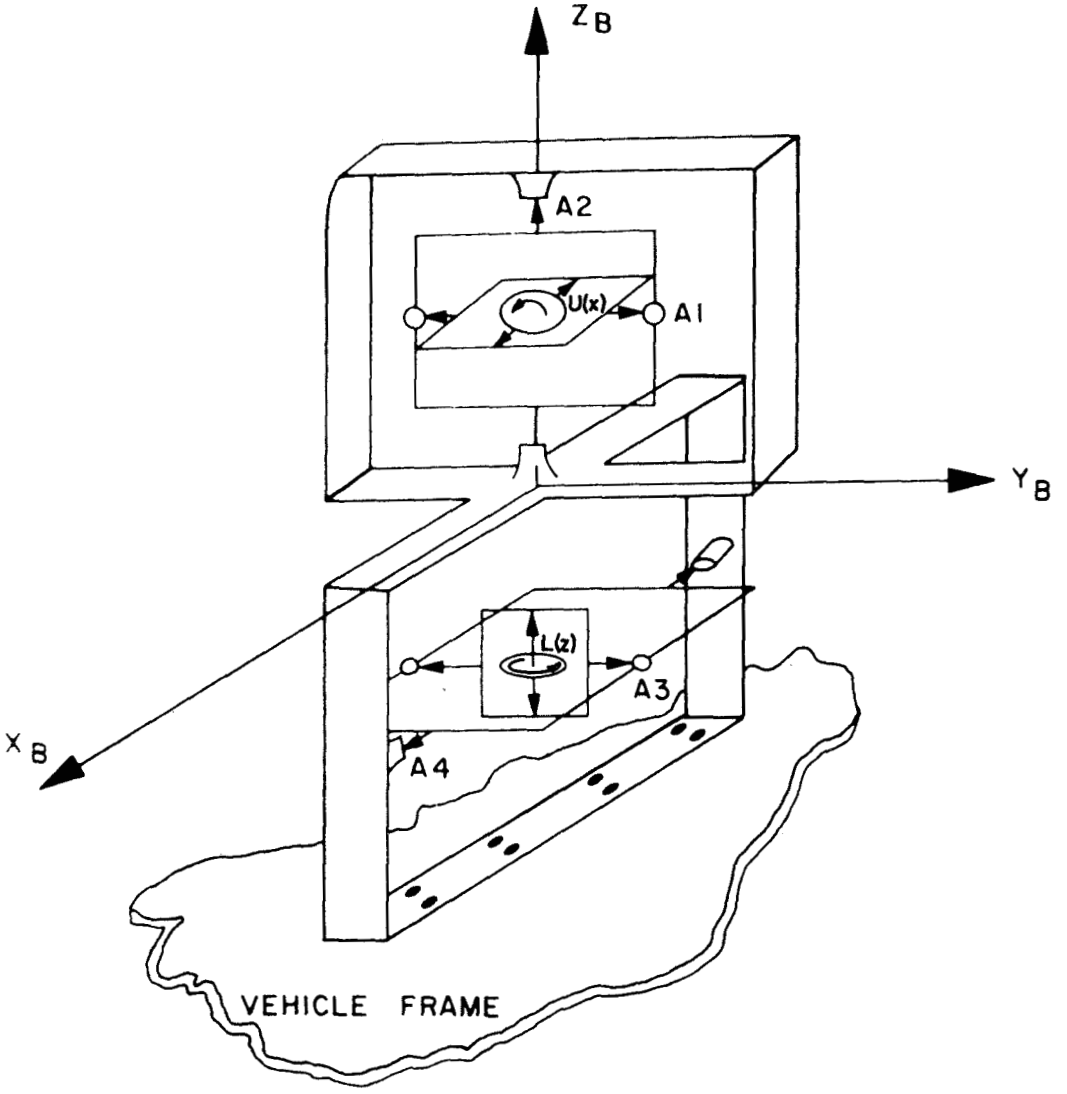

Figure 2. Two-degree-of-freedom gyros mounted to vehicle frame.

and

$$\begin{vmatrix} X \\ Y \\ Z \end{vmatrix}_B = [A4(X)]\ [A3(Y)]\ [L(Z)] \begin{vmatrix} X \\ Y \\ Z \end{vmatrix}_I . \qquad (2)$$

Therefore

$$\begin{vmatrix} X \\ Y \\ Z \end{vmatrix}_B = [T] \begin{vmatrix} X \\ Y \\ Z \end{vmatrix}_I , \qquad (3)$$

or

$$[A2(Z)]\ [A1(Y)]\ [U(X)] = [A4(X)]\ [A3(Y)]\ [L(Z)] \qquad (4)$$

The transformation components are given by

$$A1(Y) = \begin{vmatrix} \cos(A1) & 0 & -\sin(A1) \\ 0 & 1 & 0 \\ \sin(A1) & 0 & \cos(A1) \end{vmatrix} ; \quad A2(Z) = \begin{vmatrix} \cos(A2) & \sin(A2) & 0 \\ -\sin(A2) & \cos(A2) & 0 \\ 0 & 0 & 1 \end{vmatrix} ;$$

$$A3(Y) = \begin{vmatrix} \cos(A3) & 0 & -\sin(A3) \\ 0 & 1 & 0 \\ \sin(A3) & 0 & \cos(A3) \end{vmatrix} ; \quad A4(X) = \begin{vmatrix} 1 & 0 & 0 \\ 0 & \cos(A4) & \sin(A4) \\ 0 & -\sin(A4) & \cos(A4) \end{vmatrix} ;$$

$$U(X) = \begin{vmatrix} 1 & 0 & 0 \\ 0 & \cos(U) & \sin(U) \\ 0 & -\sin(U) & \cos(U) \end{vmatrix} ; \quad L(Z) = \begin{vmatrix} \cos(L) & \sin(L) & 0 \\ -\sin(L) & \cos(L) & 0 \\ 0 & 0 & 1 \end{vmatrix}$$

For simplicity, the notation $\sin(A1) = S1$, $\cos(A1) = C1$, $\sin(U) = SU$, etc. is adopted.

Note that the gimbal angle readings A1, A2, A3, and A4 are actual sequential angles. Angles U and L cannot be read directly from the gimbal angles but can be calculated (as shown later) in terms of A1, A2, A3, and A4.

From equation (4) the following expression may be written.

$$[U(X)]\,[L(Z)]^{-1} = [A1(Y)]^{-1}\,[A2(Z)]^{-1}\,[A4(X)]\,[A3(Y)] \qquad (5)$$

or

$$[U(X)]\,[L(Z)]^{-1} = \begin{vmatrix} C1 & 0 & S1 \\ 0 & 1 & 0 \\ -S1 & 0 & C1 \end{vmatrix} \begin{vmatrix} C2 & -S2 & 0 \\ S2 & C2 & 0 \\ 0 & 0 & 1 \end{vmatrix} \begin{vmatrix} 1 & 0 & 0 \\ 0 & C4 & S4 \\ -0 & -S4 & C4 \end{vmatrix} \begin{vmatrix} C3 & 0 & -S3 \\ 0 & 1 & 0 \\ S3 & 0 & C3 \end{vmatrix}$$

$$= \begin{vmatrix} C1C2 & -C1S2 & S1 \\ S2 & C2 & 0 \\ -S1C2 & S1S2 & C1 \end{vmatrix} \begin{vmatrix} C3 & 0 & -S3 \\ S4S3 & C4 & S4C3 \\ C4S3 & -S4 & C4C3 \end{vmatrix} ,$$

giving

$$[U(X)][L(Z)]^{-1} = \begin{vmatrix} C1C2C3 - C1S2S4S3 + S1C4S3 & -C1S2C4 - S1S4, & -C1C2S3 - C1S2S4C3 + S1C4C3 \\ S2C3 + C2S4S3 & C2C4 & -S2S3 + C2S4C3 \\ -S1C2C3 + S1S2S3S4 + C1C4S3 & S1S2C4 - C1S4 & S1C2S3 + S1S2S4C3 + C1C4C3 \end{vmatrix} \quad (6)$$

Also,

$$[U(X)][L(Z)]^{-1} = \begin{vmatrix} CL & -SL & 0 \\ CUSL & CUCL & SU \\ -SUSL & -SUCL & CU \end{vmatrix} \quad . \quad (7)$$

Therefore, equating (6) and (7) yields

$$CL = C1C2C3 - C1S2S4S3 + S1C4S3 \quad (8)$$

$$SL = C1S2C4 + S1S4 \quad (9)$$

$$SU = -S2S3 + C2S4C3 \quad (10)$$

$$CU = S1C2S3 + S1S2S4C3 + C1C4C3 \quad . \quad (11)$$

Let the sequence of rotation be given by equation (2). Then

$$\begin{vmatrix} X \\ Y \\ Z \end{vmatrix}_B = \begin{vmatrix} C3C1 & C3SL & -S3 \\ -C4SL + S4S3CL & C4CL + S4S3SL & S4C3 \\ S4SL + C4S3CL & -S4CL + C4S3SL & C4C3 \end{vmatrix} \begin{vmatrix} X \\ Y \\ Z \end{vmatrix}_I \quad .$$

This sequence of rotations is shown in Figure 3.

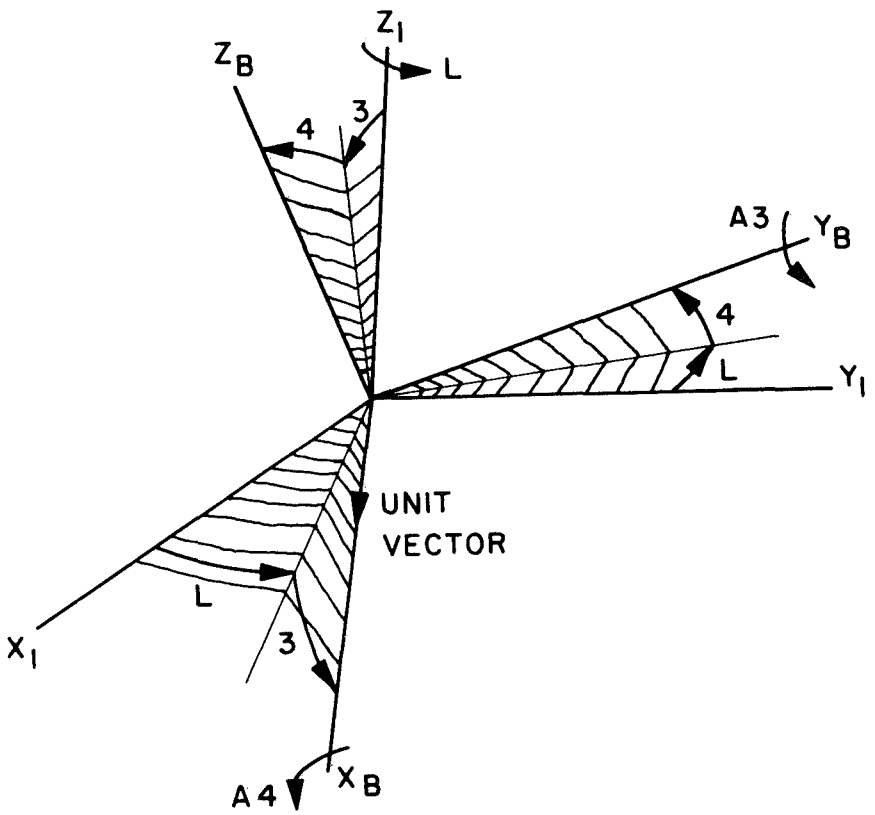

Figure 3. Sequential angle rotation defining the vehicle body axes with respect to the inertial axes.

The X_I, Y_I, Z_I components are related to the body components by

$$\begin{vmatrix} X \\ Y \\ Z \end{vmatrix}_I = \begin{vmatrix} C3CL & -C4SL + S4S3CL & S4SL + C4S3CL \\ C3SL & C4CL + S4S3SL & -S4CL + C4S3SL \\ -S3 & S4C3 & C4C3 \end{vmatrix} \begin{vmatrix} X \\ Y \\ Z \end{vmatrix}_B . \quad (12)$$

Consider a unit vector along the X body axis. This will yield the following X_I, Y_I, Z_I components.

$$X_{IC} = C3CL \tag{13}$$

$$Y_{IC} = C3SL \tag{14}$$

$$Z_{IC} = -S3 \tag{15}$$

Define the pitch angle of the vehicle with respect to the X_I, Y_I, Z_I frame to be α. Define the bearing angle of the vehicle with respect to the reference bearing line to be β. It follows that

$$\tan \alpha = \frac{-Z_{IC}}{\sqrt{X_{IC}^2 + Y_{IC}^2}}$$

where X_{IC}, Y_{IC}, and Z_{IC} are given in equations (13), (14), and (15), respectively. Therefore,

$$\tan \alpha = \frac{S3}{\sqrt{C3^2CL^2 + C3^2SL^2}}$$

or

$$\tan \alpha = \tan 3$$

and

$$\text{angle } \alpha = \text{angle } 3 \tag{16}$$

Although this result is no great surprise, it is significant that the pitch angle can be determined by direct reading of gimbal angle A3.

The bearing angle is given by

$$\tan \beta = \frac{Y_{IC}}{X_{IC}} = \tan L$$

or

$$\text{angle } \beta = \text{angle } L$$

From equations (8) and (9) one finds that

$$\text{angle } L = \tan^{-1}\left[\frac{C1S2C4 + S1S4}{C1C2C3 - C1S2S4S3 + S1C4S3}\right] , \qquad (17)$$

so that the bearing angle is defined in terms of the gimbal angle readings A1, A2, A3, and A4.

Another angle of interest is the angle from the vehicle heading reference to the point location of the LRV projected onto the X_I, Y_I plane. This angle is illustrated in Figure 4. It is desired to know the angle that the vehicle must head to return to the LEM location. We define this angle in Figure 5. The angle ϕ, defined as the counterclockwise rotation from the X_I, Y_I projected heading of the vehicle, gives the desired angle. For the general case,

$$\beta + \phi - \theta = 180 \text{ degrees} ,$$

or

$$\phi = 180 + \theta - \beta \qquad (18)$$

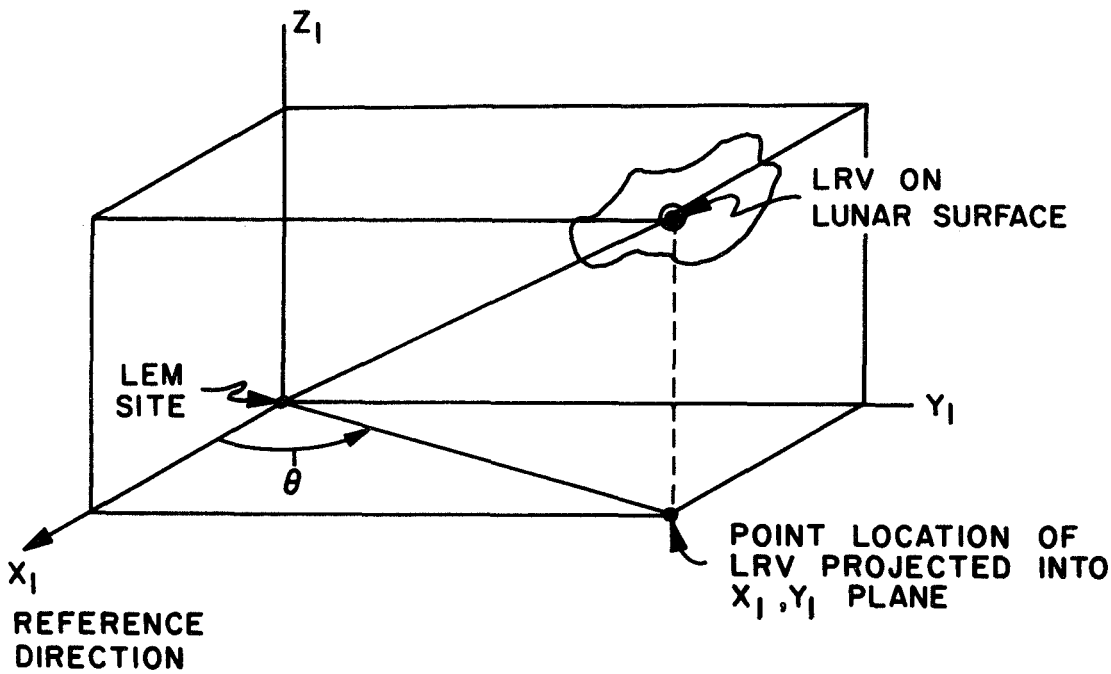

Figure 4. Angle between the reference direction and projection of LRV location onto X_I, Y_I plane.

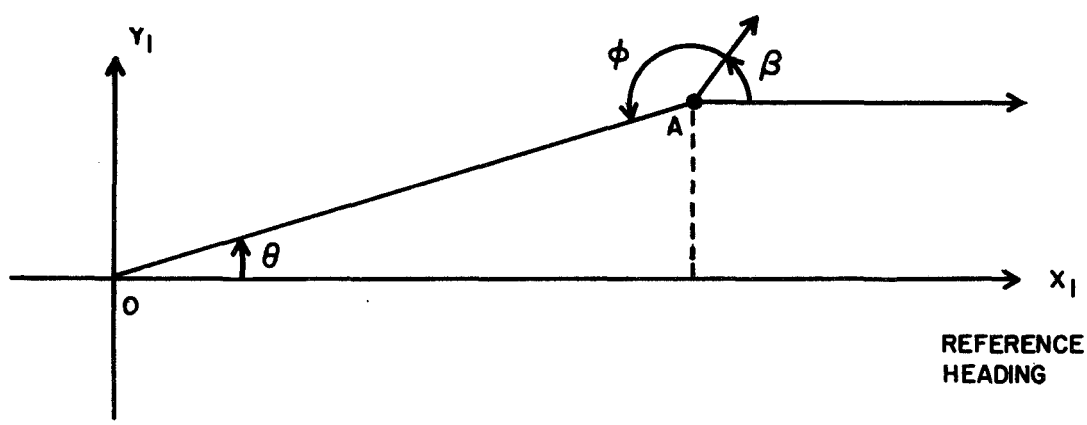

Figure 5. Heading angle to LEM

where

$$\theta = \tan^{-1} \frac{[Y_I]}{X_I} \tag{19}$$

With the information given in equations (16), (17), and (18), navigation requirements can be satisfied. A block diagram of the navigation system is shown in Figure 6. For convenience the displayed quantities are defined.

S	- Total distance traveled by the LRV
$\dot{S}$	- Velocity of LRV
R	- Radial distance traveled by the vehicle
β	- Bearing angle of the vehicle with respect to the reference bearing
ϕ	- Heading angle of the vehicle back to LEM
X_I, Y_I, Z_I	- Distance traveled by the vehicle with respect to the moon-fixed inertial system whose origin rotates with the moon.

SIMULATION CONSIDERATIONS

To determine the range of required quality of the gyros and acceptable system misalignments, error analysis for the navigation system must be made. The details of how a digital simulation of the navigation system can be used to perform this error analysis are as follows.

Outline of Simulation Study

We first consider the effects of gyro drift errors. These errors, when multiplied by time, are reflected in the gimbal angle readings of A1, A2, A3, and A4. The following method is used to assess the effects of gyro drift rates.

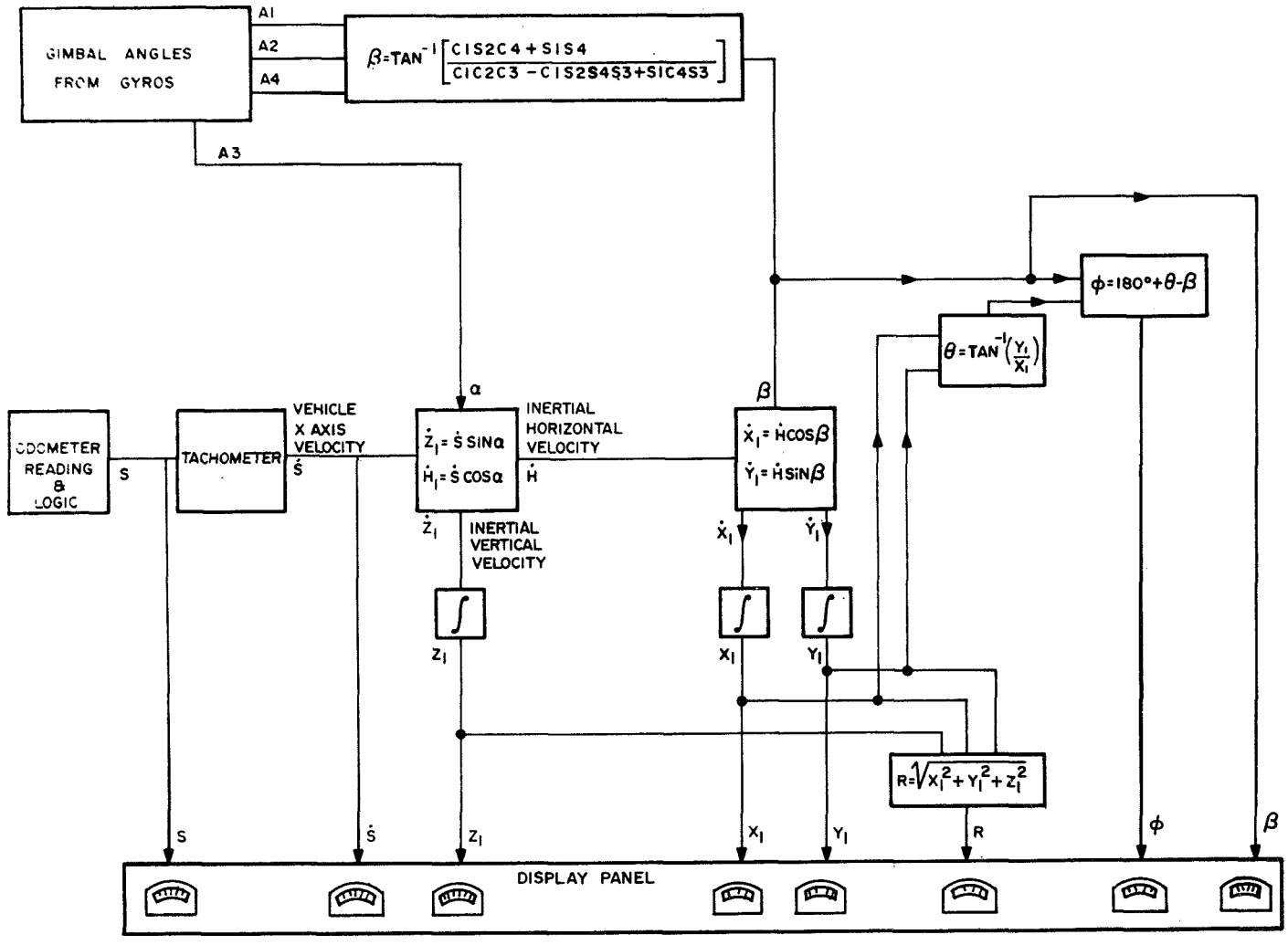

Figure 6. Block diagram of proposed navigation system.

Step 1. Assume a velocity profile for the vehicle. This velocity is denoted by $\dot{S}$.

Step 2. Assume a set of sequential angles, in particular the angle sequence given in Figure 3, corresponding to the velocity profile in Step 1.

Step 3. From the rotation sequence in Step 2, develop the expressions for determining A1, A2, A3, and A4 as a function of the angles in Step 2.

Step 4. Write a digital simulation program for the navigation system given in Figure 6. The inputs to the program will be $\dot{S}$ and A1, A2, A3, and A4.

Step 5. Run the simulation for a specified time, T_{total}. The following information will be printed out every ΔT seconds: time, X_I, Y_I, Z_I, β, ϕ, and R. These printouts will establish a reference set of data to be compared with future runs which include drift rate errors.

Step 6. Introduce a set of known drift rates into A1, A2, A3, and A4 as given in Step 3.

Step 7. Run the simulation for the same velocity profile as given in Step 1. Print out the same data at the same ΔT as produced in Step 5.

Step 8. Compare the results of Step 7 with Step 5 to determine the effect of errors introduced by the drift rates. These errors should be compared with the required system accuracy specifications as previously given.

Step 9. Repeat Steps 6, 7, and 8 for as many combinations of drift rates as desired.

To assess the effects of misalignments, a similar approach to that outlined in Steps 1 through 9 can be employed. There are two major sources of misalignment errors. First, the two gyros may be physically misaligned with respect to the vehicle frame. The misalignment of the upper gyro is independent of the lower gyro. Second, on any given sortie, the vehicle may not be aligned precisely as it was on previous sorties. This means that an error will exist with respect to locating previously established sites.

Hardware misalignments can be held to within 30 arc seconds by careful alignment procedures. Since these errors are small compared to vehicle misalignments, they will be neglected.

Vehicle misalignment errors can easily be evaluated by specifying the sequential angles L, A3, and A4 corresponding to the desired misalignment to be evaluated. These misalignment angles are introduced in Step 6 of the error evaluation procedure.

Background Analysis for Simulation Inputs

This section concerns the problems of selecting a velocity profile $\dot{S}$ for Step 1, selecting a body rotation sequence (as a function of time) for Step 2, and developing the expressions for determining the angles A1, A2, A3, and A4 as a function of the sequential angles. First, the relationships between the angles will be developed.

The rotation sequence selected is given in equation (1) and shown in Figure 3. The first rotation is around the Z_B axis by an angle L, the second rotation is around the Y_B axis by an angle A3, and the third rotation is around the X_B axis by an angle A4. Note that the sequential angles A3 and A4 are the same angles A3 and A4 as read by the lower gyro gimbals in Figure 2. It has been shown that if angles A1, A2, A3, and A4 are given, then the sequential angles L, A3, and A4 can be determined. Actually the only angle to be determined is angle L, and it may be determined from equations (8) and (9). Now to make the relationship between the sequential angles and the gimbal angles bilateral, expressions for A1 and A2 must be determined as a function of angles L, A3, and A4.

The transformation matrix between the inertial axis and the body axes can be written as

$$T = \begin{vmatrix} C2C1 & C2S1SU + S2CU & -C2S1CU + S2SU \\ -S2C1 & -S2S1SU + C2CU & S2S1CU + C2SU \\ S1 & -C1SU & C1CU \end{vmatrix} , \qquad (20)$$

or

$$T = \begin{vmatrix} C3CL & C3SL & -S3 \\ -C4SL + S4S3CL & C4CL + S4S3SL & S4C3 \\ S4SL + C4S3CL & -S4CL + C4S3SL & C4C3 \end{vmatrix} \tag{21}$$

Therefore, equating equation (20) to (21) and solving for A1 and A2 yields

$$A1 = \sin^{-1} [S4SL + C4S3CL] \tag{22}$$

and

$$A2 = \tan^{-1} \frac{[C4SL - S4S3CL]}{C3CL} \tag{23}$$

Thus, with knowledge of the sequential angles L, A3, and A4, the gimbal angles A1, A2, A3, and A4 are known and this completes the bilateral relationship.

Vehicle Velocity and Position Profile for Error Analysis

The vehicle velocity and position profile can be arbitrarily selected. However, this method may lead to unrealistic vehicle position. For example, the vehicle may be traveling upside down. To avoid this, a profile will be selected so that the position and velocity of the vehicle are approximately known as a function of time. The profile selected is shown in Figure 7 and is divided into five segments as indicated. The following information describes each segment.

Segment 1. Over segment 1 the vehicle has a linear velocity given by

$$\dot{S} = 30t \text{ km/hr} \qquad (0 \leq t \leq 0.3 \text{ hr})$$

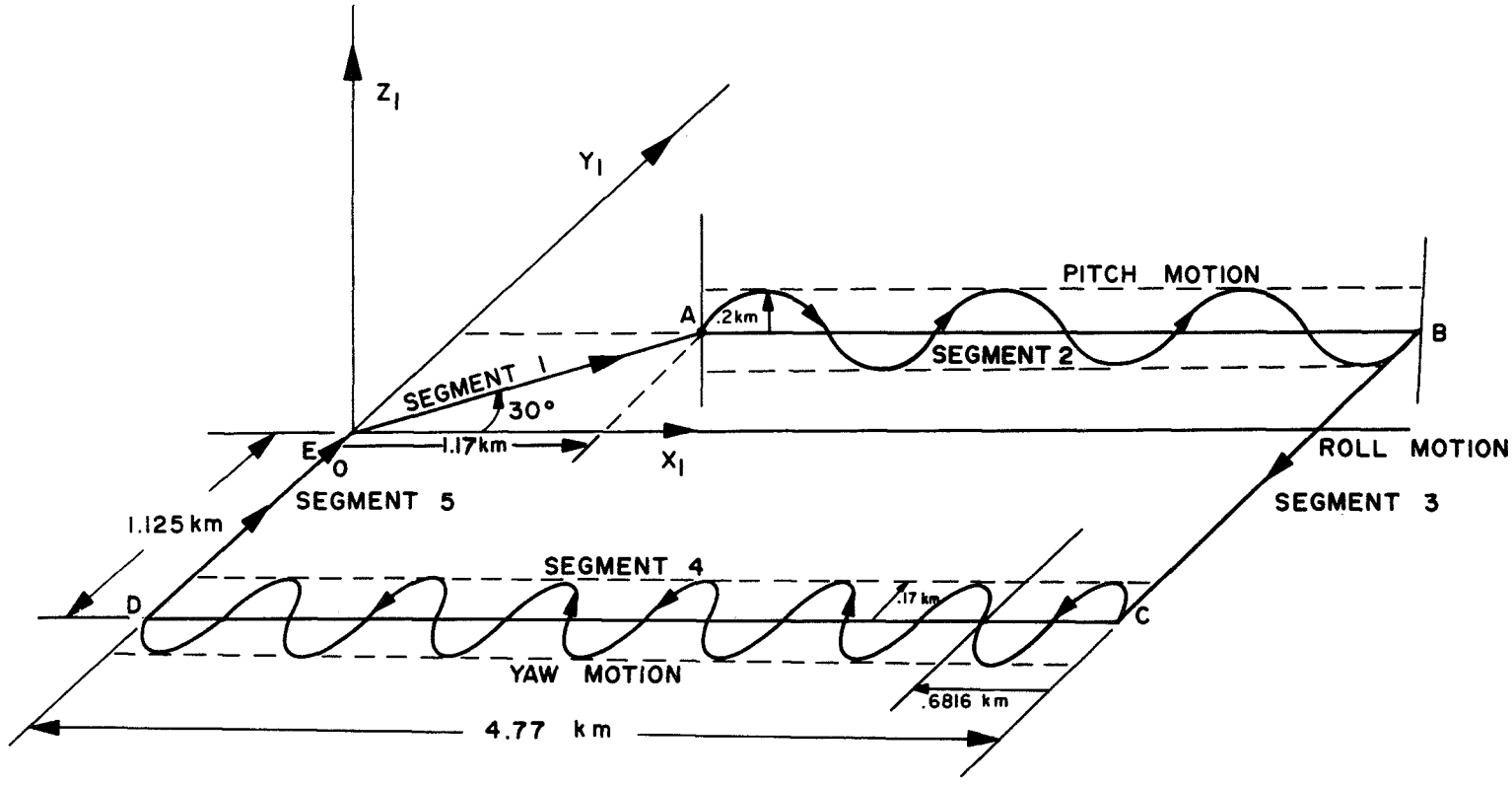

Figure 7. Selected vehicle profile for error analysis.

The heading of the vehicle is at a constant 30 degrees so that

angle L = +30 degrees

angle A3 = 0 degree

angle A4 = 0 degree

The total distance traveled is

$$S = 1.35 \text{ km}$$

At t = 0.3 hr, the velocity of the vehicle will be 9 km/hr and the coordinates of point A will be

$$X_I = 1.17 \text{ km}, \qquad Y_I = 0.675 \text{ km}, \qquad Z_I = 0 \text{ km}$$

The gimbal angles A1 and A2 are determined from equations (22) and (23), respectively.

A1 = 0 degree, A2 = 30 degrees .

Segment 2. Over segment 2 the vehicle has a constant velocity of

$$\dot{S} = 9 \text{ km/hr} \qquad (0.3 \leq t \leq 0.796 \text{ hr})$$

The vehicle has a constant 0-degree heading, but a sinusoidal pitch profile as shown in Figure 8. The distance traveled along the sinusoidal path is given by

$$S = \frac{12}{M} \int_0^{\sigma} \sqrt{1 + K_1^2 M^2 \cos^2 MX} \; d(MX) \qquad (22)$$

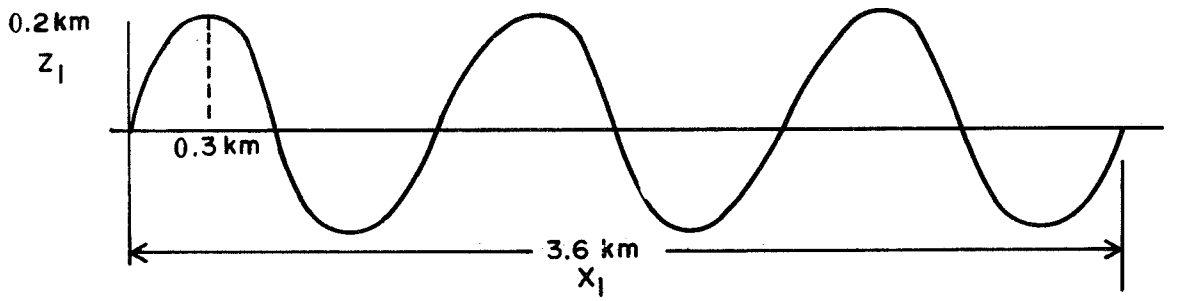

Figure 8. Pitch profile for segment 2 of vehicle path.

where $K_1 = 0.2$ km; $M = 5.23$. Equation (22) can be put into the elliptic integral form

$$S = A \int_0^{\sigma} \sqrt{1 - K^2 \sin^2 \psi} \quad d\psi$$

where

$$K = \sqrt{\frac{K_1^2 M^2}{1 + k_1^2 M^2}} \quad ,$$

$$A = \frac{12\sqrt{1 + K_1^2 M^2}}{M}$$

The approximate evaluation of this elliptic integral of the second kind gives

$$S = 4.464 \text{ km}$$

The sequential angles are given by

angle L = 0 degree

angle A4 = 0 degree

angle A3 = 46.3 degrees $\cos\left(\frac{9\pi}{0.744}\ t'\right)$

The gimbal angles A1 and A2 are

$$A1 = 46.3 \text{ degrees } \cos\left(\frac{9\pi}{0.744}\, t'\right)$$

$$A2 = 0$$

where

$$(t' = t - 0.3)$$

The X_I, Y_I, Z_I coordinates at point B are approximately

$$X_I = 4.77 \text{ km}, \quad Y_I = 0.675 \text{ km}, \quad Z_I = 0 \text{ km} \quad .$$

Segment 3. The velocity of the vehicle is constant over this segment and given by

$$\dot{S} = 9 \text{ km/hr} \qquad (0.796 \leq t \leq 0.996)$$

The heading of the vehicle is a constant -90 degrees. The distance traveled is

$$S = 1.8 \text{ km}$$

The vehicle has a sinusoidal roll motion of

$$30 \text{ degrees } \sin(100\pi t'')$$

$$t'' = t - 0.796 \qquad (0.796 \leq t \leq 0.996)$$

The sequential angles are given by

angle L = -90 degrees

angle A3 = 0 degree

angle A4 = 30 degrees sin ($100\pi t''$) .

The gimbal angles A1 and A2 are

A1 = -30 degrees sin ($100\pi t''$)

A2 = -90 degrees .

The X_I, Y_I, Z_I coordinates at point C are

X_I = 4.77 km, Y_I = -1.125 km, Z_I = 0 km .

Segment 4. The vehicle velocity is constant over this segment and given by

$\dot{S}$ = 5.01 km/hr $(0.996 \leq t \leq 2.39)$

The pitch and roll angles of the vehicle are zero and the yaw profile is shown in Figure 9. The length of the path can be evaluated as an elliptic integral of the second kind and yields

S = 7.0 km .

The sequential angles are given by

angle L = 180 degrees - 57.5 degrees cos ($31.506t'''$) ($t''' = t - 0.996$).

angle A3 = 0 degree

angle A4 = 0 degree

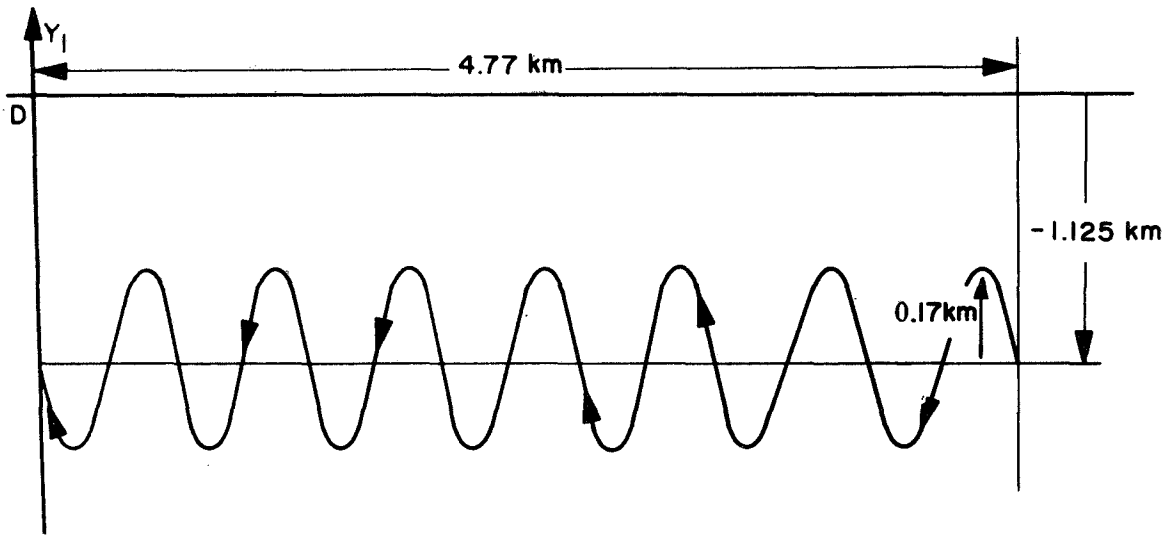

Figure 9. Yaw profile for segment 4 of vehicle path.

The gimbal angles A1 and A2 are

$$A1 = 0 \text{ degree}$$

$$A2 = 180 \text{ degrees} - 57.5 \text{ degrees} \cos(31.506t''')$$

The X_I, Y_I, Z_I coordinates at point D are approximately

$$X_I = 0 \text{ km}, \quad Y_I = -1.125 \text{ km}, \quad Z_I = 0 \text{ km}$$

Segment 5. The vehicle velocity is constant over this segment and given by

$$\dot{S} = 1.85 \text{ km/hr} \qquad (2.39 < t \leq 3.0)$$

The sequential angles are

angle L = 90 degrees

angle A3 = 0 degree

angle A4 = 0 degree

The gimbal angles A1 and A2 are

A1 = 0 degree

A2 = 90 degrees

The X_I, Y_I, Z_I coordinates at point E are approximately all zero.

The answers for all segments above are only approximate. The actual values with zero system errors are given by the computer simulation results.

A DIGITAL SIMULATION OF THE NAVIGATION SYSTEM

A block diagram of the navigation system is shown in Figure 6. This block diagram is used as the starting point for writing the simulation program. It should be pointed out that Figure 6 shows the complete set of calculations required for this navigation system. On the other hand, the digital simulation will require additional calculations. In particular the angles A1, A2, A3, and A4 are direct inputs to the actual system, but these same quantities must be calculated as a function of time in the digital simulation. Also, a capability must be included in the digital program for simulating system errors.

A flow chart of the simulation program written for this navigation system is shown in the Appendix. The actual program was written in Fortran and the quantities given in the program listing (Appendix) were modified to be compatible with Fortran requirements.

SIMULATION RESULTS

Using the surface profile shown in Figure 7, a simulation run was first made without system errors to establish a set of reference data. The results are in good agreement with the analytical approximations given previously and therefore validate the computer simulation.

Graphs showing the reference data for X_I, Y_I, Z_I, β, ϕ, and R versus time are given in Figures 10 through 15, respectively. For convenience, the definitions of these quantities are given below.

X_I, Y_I, Z_I - Distances traveled by the vehicle with respect to the moon-fixed inertial coordinate system. The origin of the moon-fixed coordinate system is located near the LEM and moves with the lunar surface.

β - The angle between the reference direction (X_I axis) and the direction of travel of the vehicle.

ϕ - The angle between the direction of travel of the vehicle and the shelter site.

R - The straight line distance between the shelter site and the LRV.

All subsequent computer simulation runs with gyro drift rates and vehicle misalignments are compared to the reference data.

Table 1 gives a summary of the simulated system errors. Various cases for gyro drift rates and vehicle misalignments were simulated. These cases are representative of the expected range of errors but do not include all possible combinations in this range. To cover the entire spectrum would require an extensive number of computer runs. However, from the cases studied one can establish trends on the accuracy of the navigation system as a function of system errors.

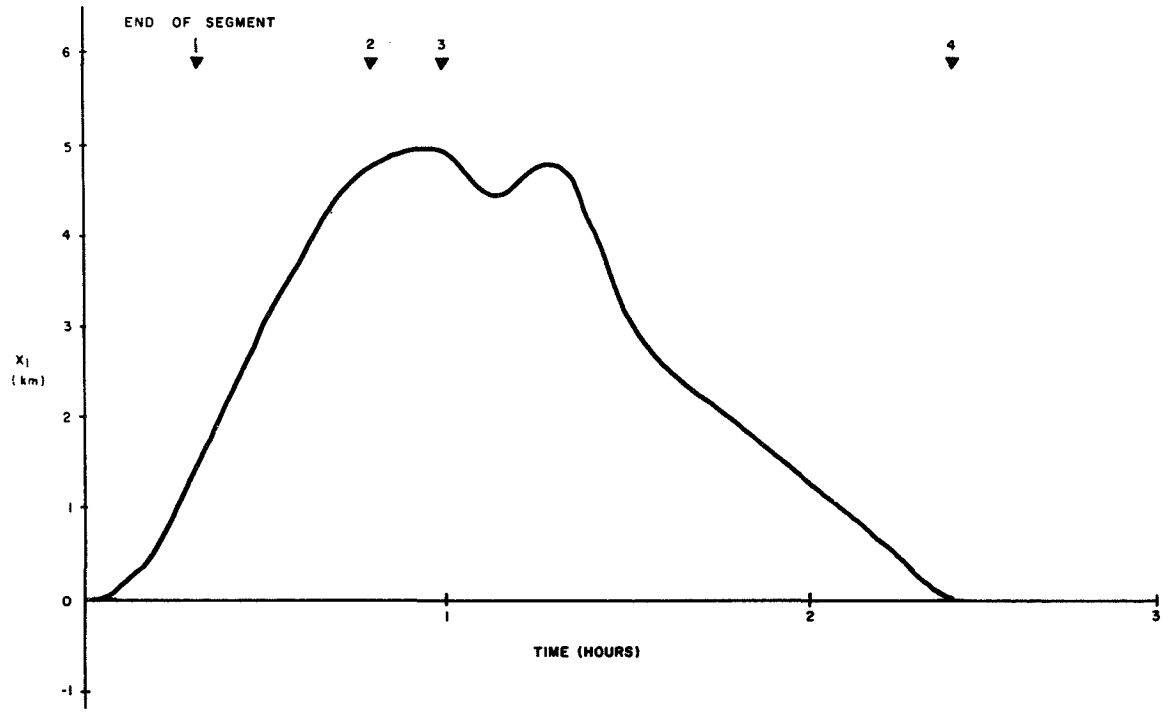

Figure 10. X_I versus time for reference trajectory.

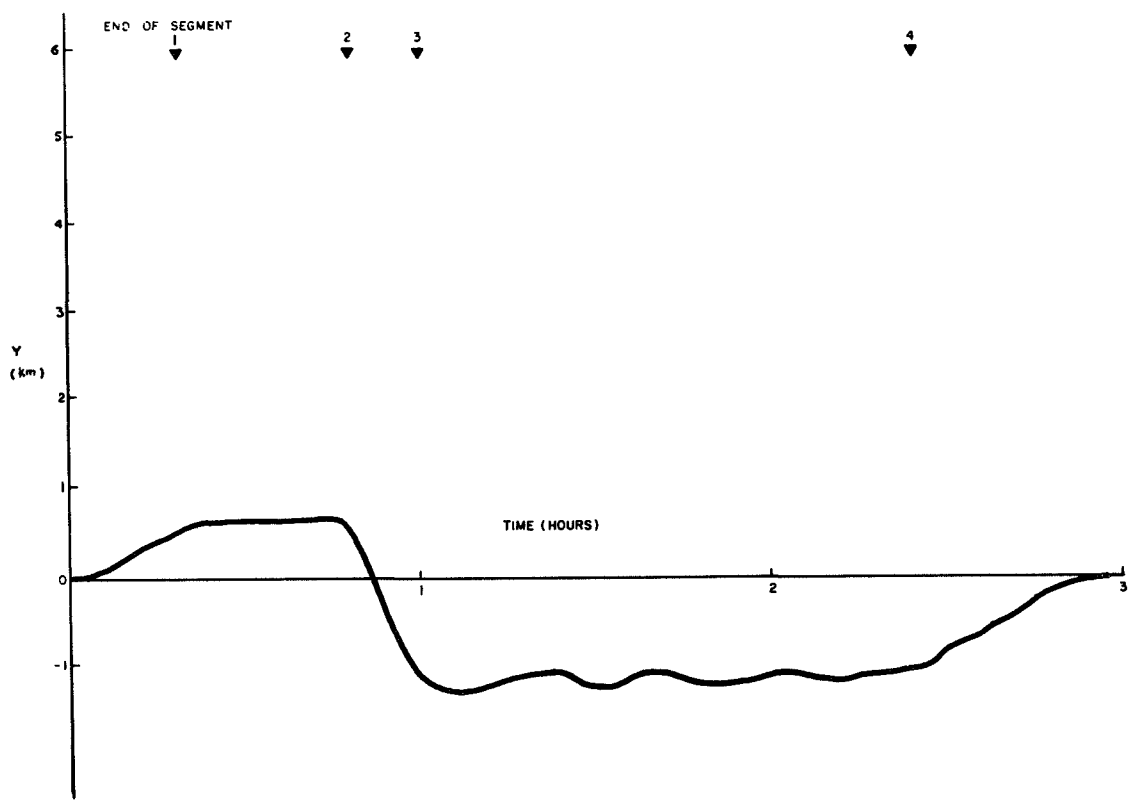

Figure 11. Y_I versus time for reference trajectory.

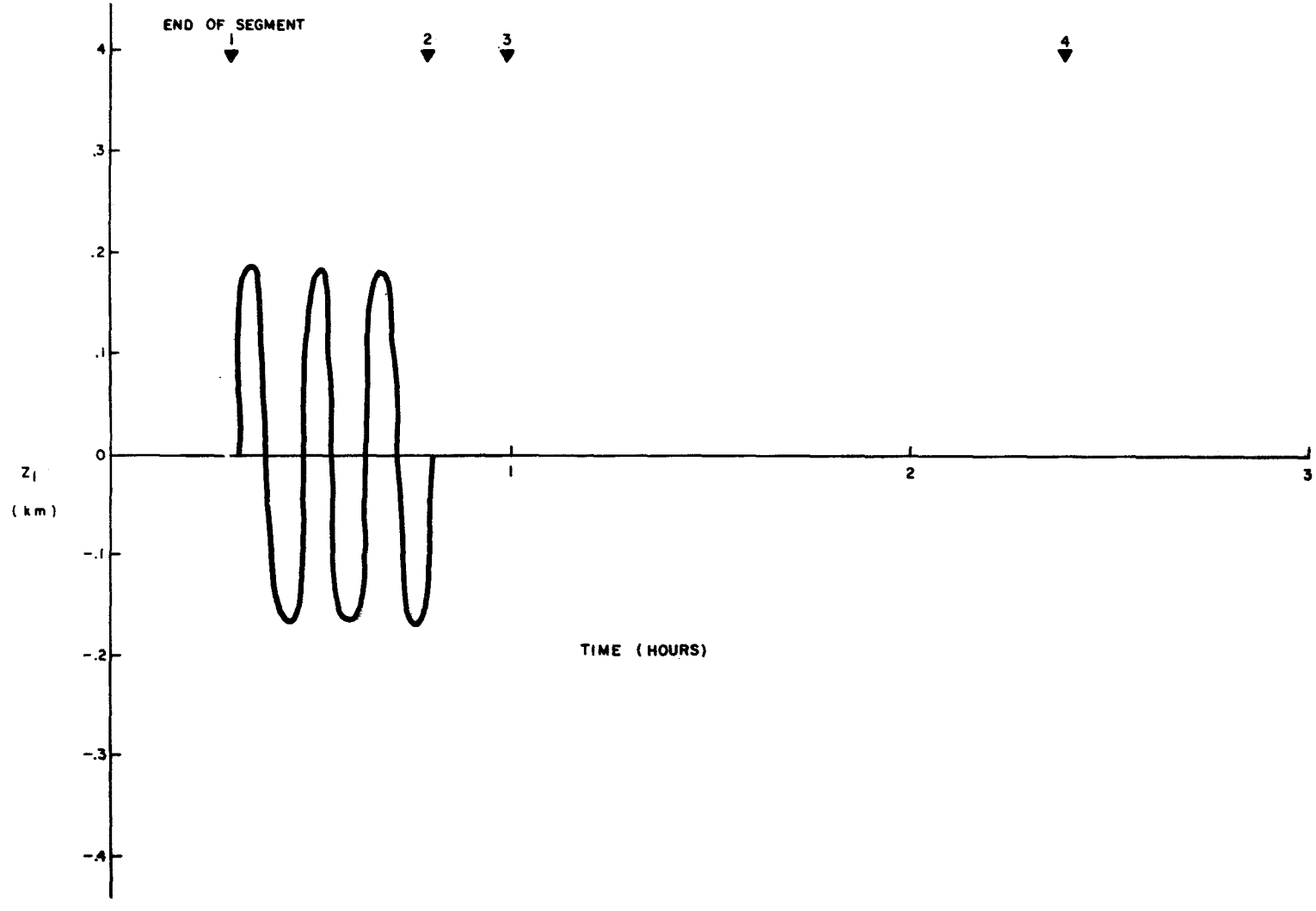

Figure 12. Z_I versus time for reference trajectory.

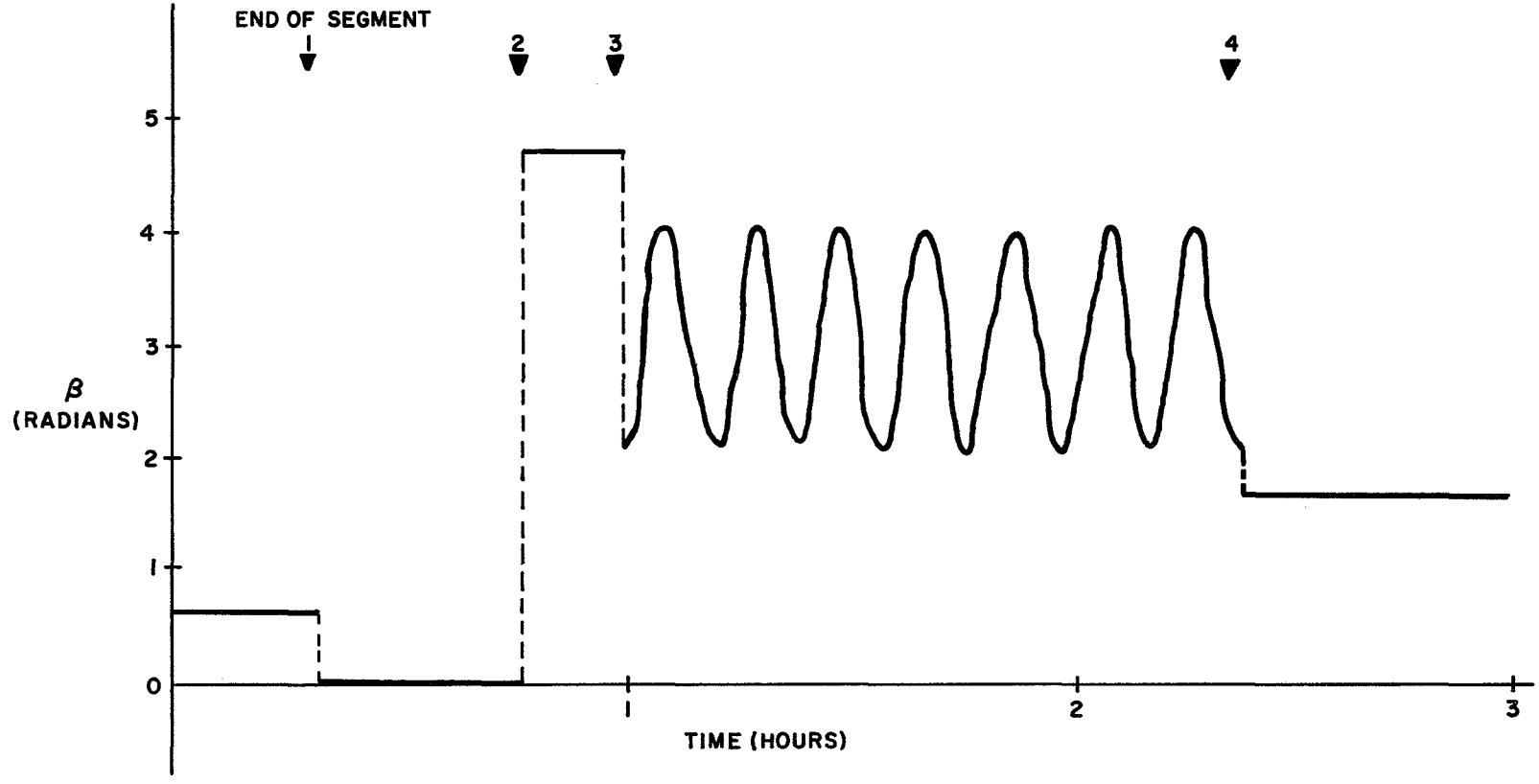

Figure 13. Beta versus time for reference trajectory.

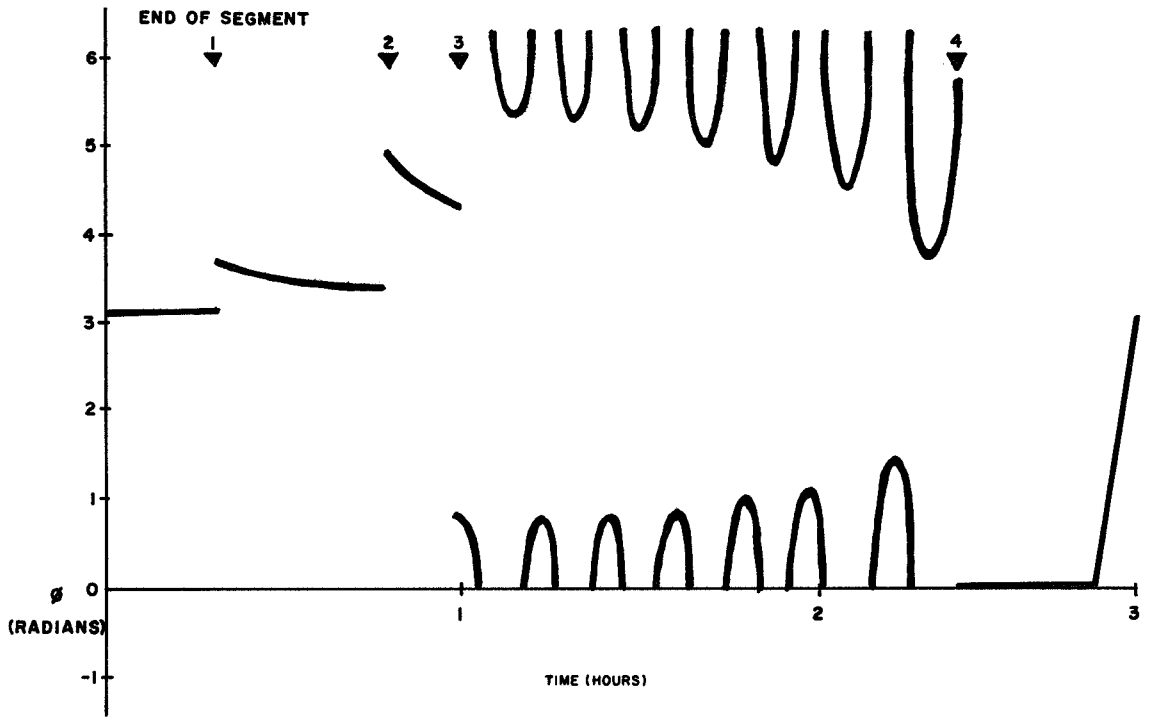

Figure 14. ϕ versus time for reference trajectory.

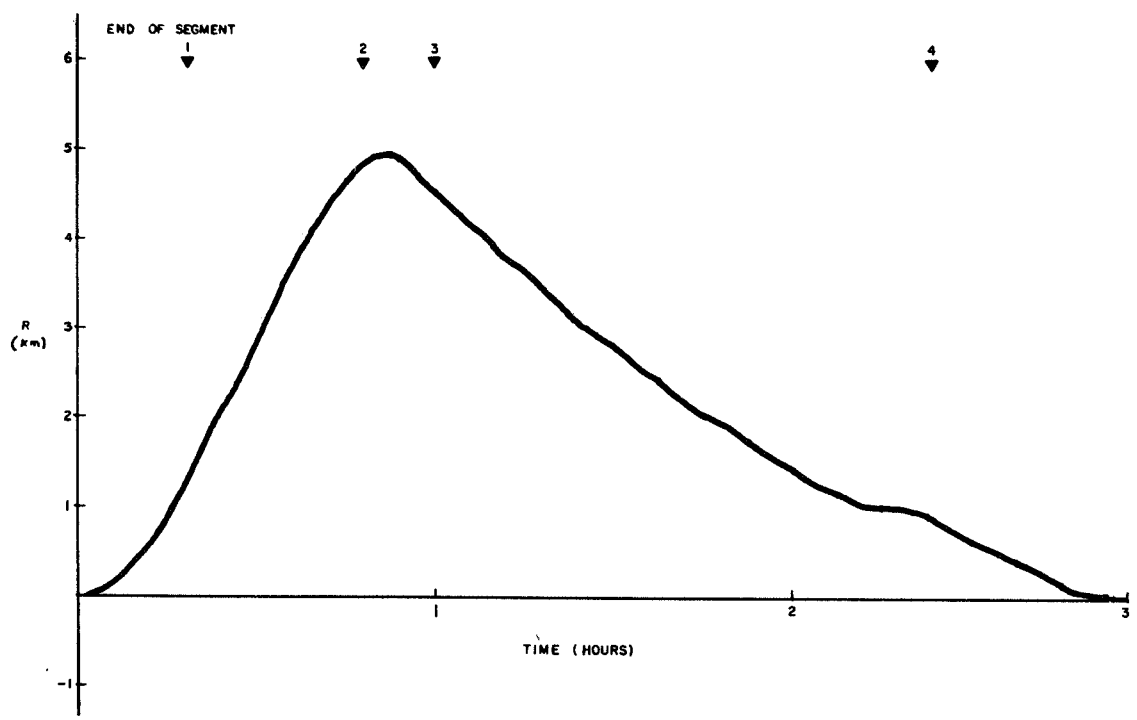

Figure 15. Range versus time for reference trajectory.

TABLE 1. SYSTEM ERRORS FOR SIMULATION STUDY

Figure Number	Case	Drift Rate Errors (degrees/hour)				Vehicle Misalignments (degrees)		
		Gimbal A1	Gimbal A2	Gimbal A3	Gimbal A4	Angle A3	Angle A4	Angle L
17	1	+1	+1	+1	+1	0	0	0
18	2	+2	+2	+2	+2	0	0	0
19	3	+3	+3	+3	+3	0	0	0
20	4	-1	-1	-1	-1	0	0	0
21	5	-2	-2	-2	-2	0	0	0
22	6	-3	-3	-3	-3	0	0	0
23	7	+1	-1	+1	-1	0	0	0
24	8	-1	+1	-1	+1	0	0	0
25	9	-1	-1	+1	+1	0	0	0
26	10	+2	-1	+2	-2	0	0	0
27	11	-2	+2	-2	+2	0	0	0
28	12	-2	-2	+2	+2	0	0	0
30	13	0	0	0	0	+1	+1	+1
31	14	0	0	0	0	-1	-1	-1
32	15	0	0	0	0	+3	+3	+3
33	16	0	0	0	0	-3	-3	-3
34	17	+1	+1	+1	+1	+1	+1	+1
35	18	+1	+1	+1	+1	+3	+3	+3
36	19	-1	-1	-1	-1	+1	+1	+1
37	20	-1	-1	-1	-1	+3	+3	+3
38	21	+1	+1	+1	+1	+1	-2	+3
39	22	0	0	0	0	+5	+5	+1
40	23	0	0	0	0	+4	+10	+1

Figure 16 shows a plot of the error in returning to the LEM site as a function of gyro drift rates. Drift rates in gimbal angles A1, A2, A3, and A4 are of equal magnitude and sign. The end point error is practically the same for either positive or negative drift rate polarity. The error in returning to the shelter site varies linearly with the gyro drift rates. The diagram shows that the vehicle will return to within a 500-meter spherical range (the maximum allowable error) for drift rates up to 1.5 degrees/hour. However, if only in-plane errors are considered, the vehicle will return within a 500-meter circle for drift rates up to 4.8 degrees/hour. For all cases, the major contributing factor to the end point error is the Z_I component. In making any closed trajectory, the error accumulation in the Z_I axis is monotonic. On the other hand, the accumulative errors in the X_I and Y_I axes have a tendency to balance out because the trajectory returns to the starting point, forming a closed path.

From a physical standpoint, the vehicle is restricted to the surface of the moon. If the endpoint errors in X_I and Y_I are small, the vehicle will be physically close to the starting point regardless of Z_I errors. However, if one is attempting to determine the altitude of the vehicle, errors in Z_I become serious.

In Table 1, cases 1 through 12 are for gyro drift rates only. Vehicle misalignments are zero for these cases. Figures 17 through 28 show the error in the angle back to the LEM site for the respective cases. The nature of this error angle should be explained.

For the first simulation run, the vehicle follows the reference trajectory with a given velocity profile without any system errors. The angle ϕ from the heading of the vehicle to the LEM site is calculated as a function of time. A second simulation run is made with gyro drift rates (multiplied by time) added to the gimbal angle readings. In this case the vehicle physically follows the same reference trajectory of the first simulation run. In other words, the vehicle pilot can visually navigate, without the aid of the navigation system, along the tracks made by the reference trajectory. Consider that the vehicle is within visual range of the LEM and located at point A on the reference trajectory shown in Figure 29. The pilot can observe that he must turn the vehicle through an angle ϕ_A to head directly to the LEM. However, the information from the navigation system may locate the vehicle at point B

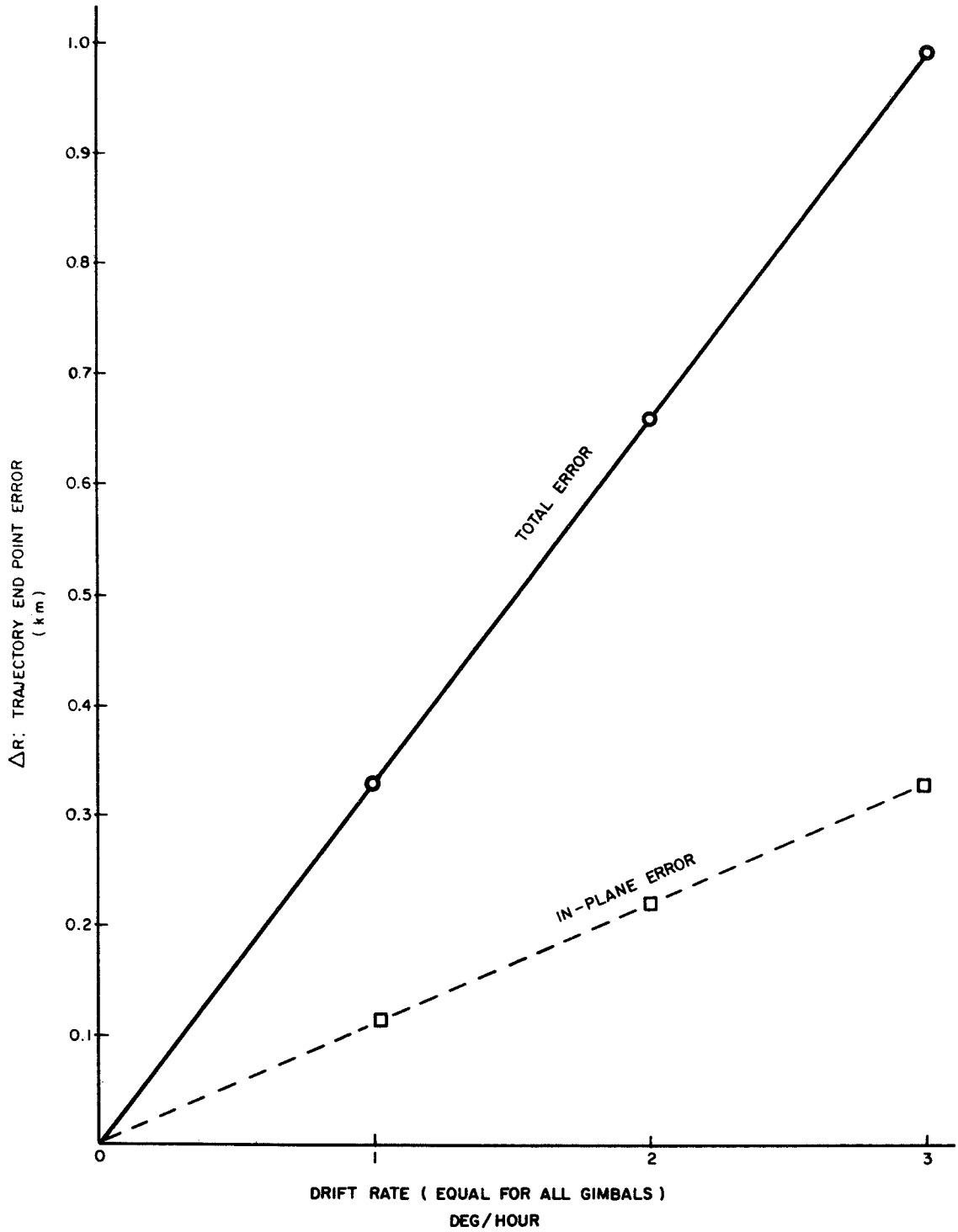

Figure 16. Trajectory end point error for gyro drift rates.

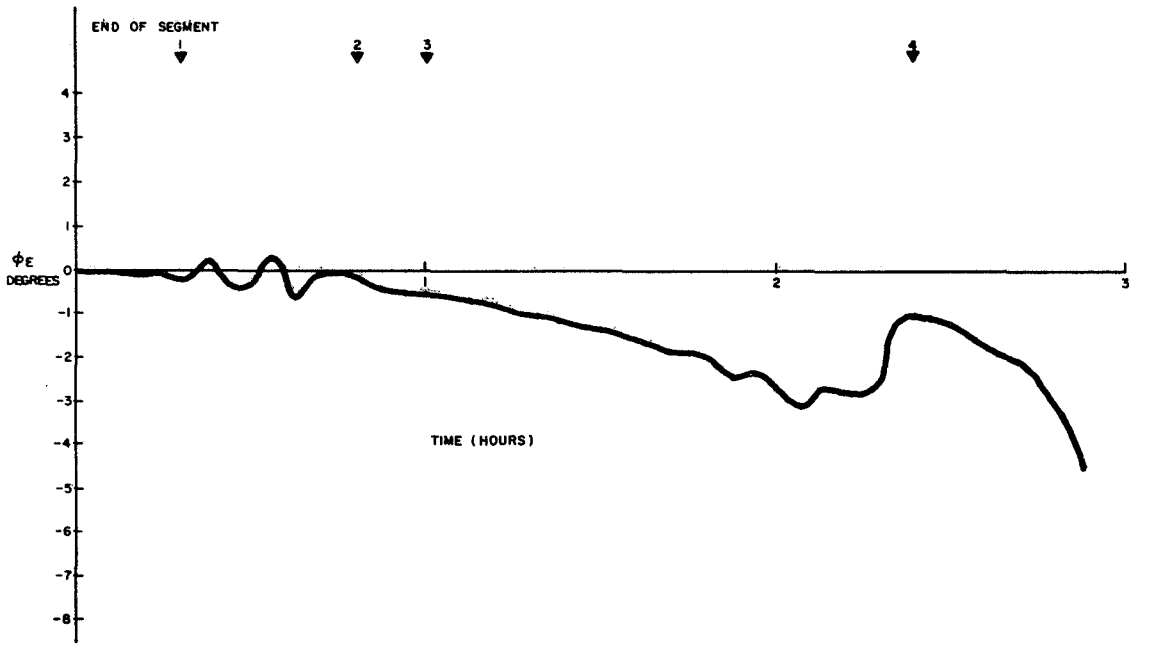

Figure 17. Bearing angle error for drift rates of A1 = +1, A2 = +1, A3 = +1, A4 = +1 deg/hour.

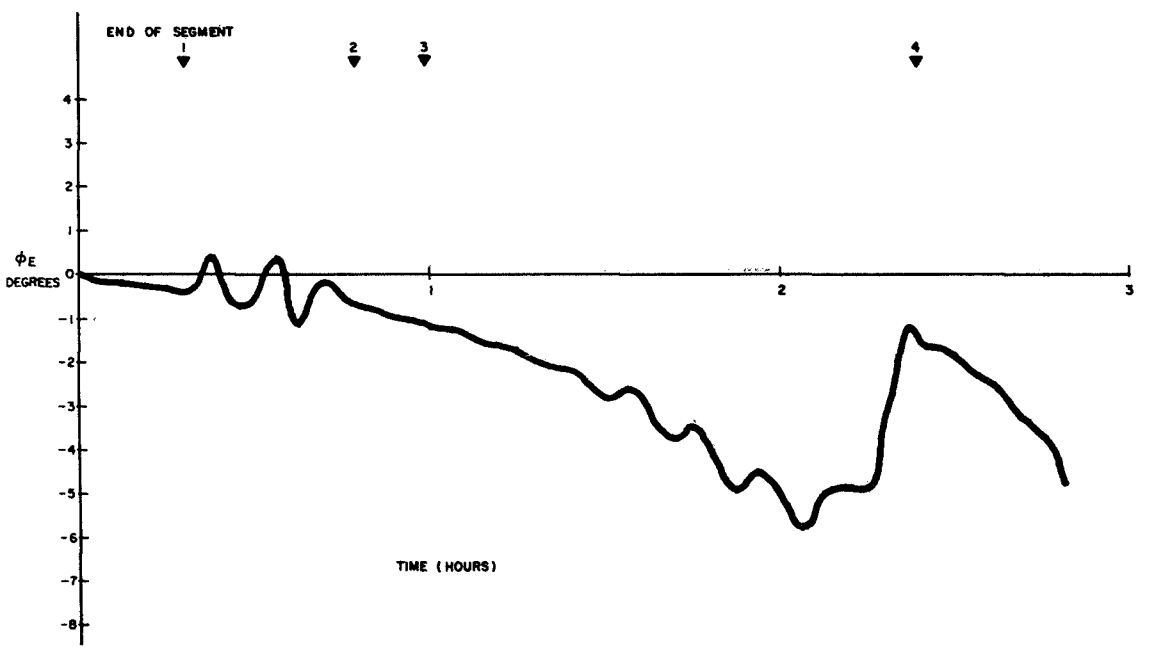

Figure 18. Bearing angle error for drift rates of A1 = +2, A2 = +2, A3 = +2, A4 = +2 deg/hour.

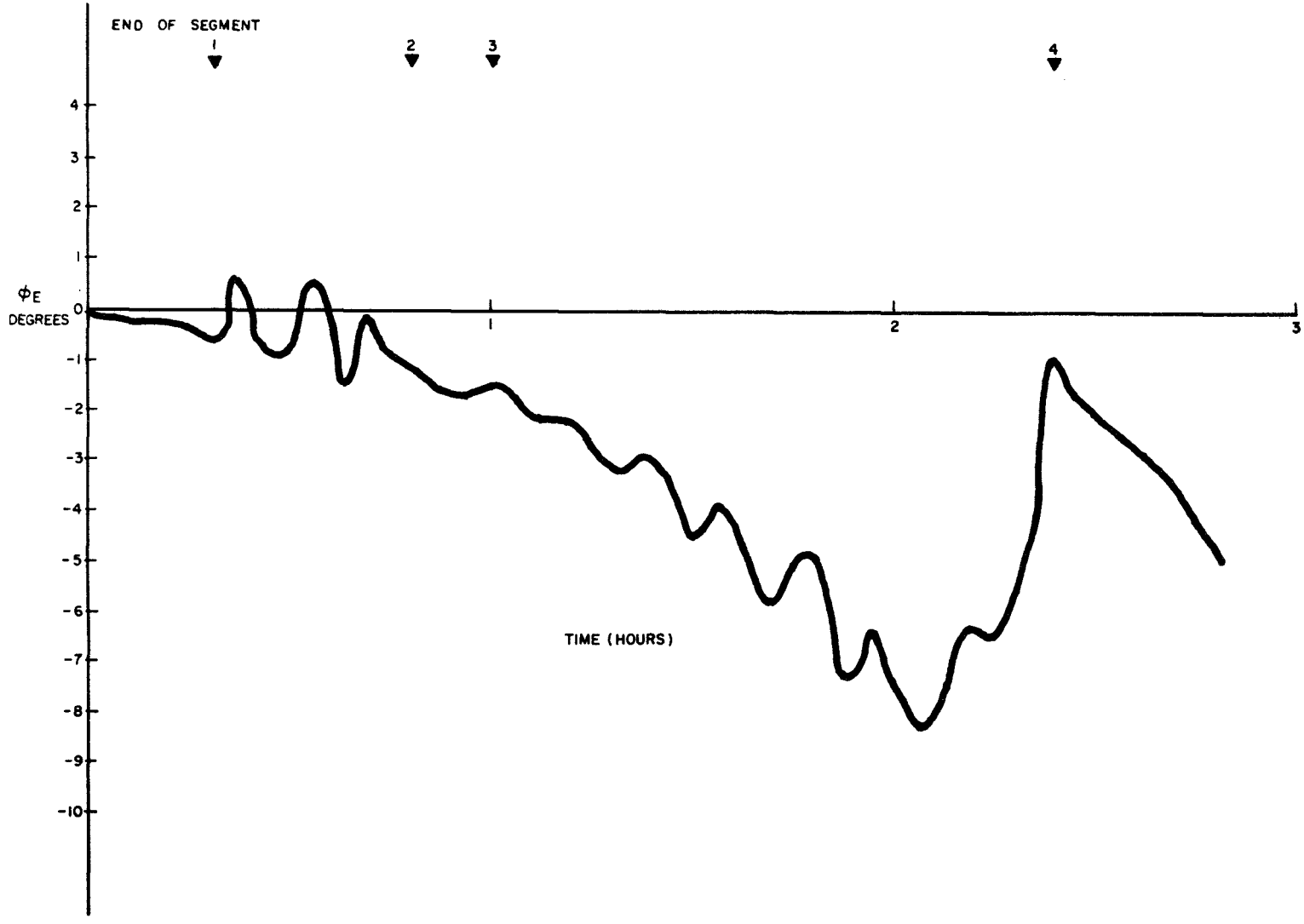

Figure 19. Bearing angle error for drift rates of A1 = +3, A2 = +3, A3 = +3, A4 = +3 deg/hour.

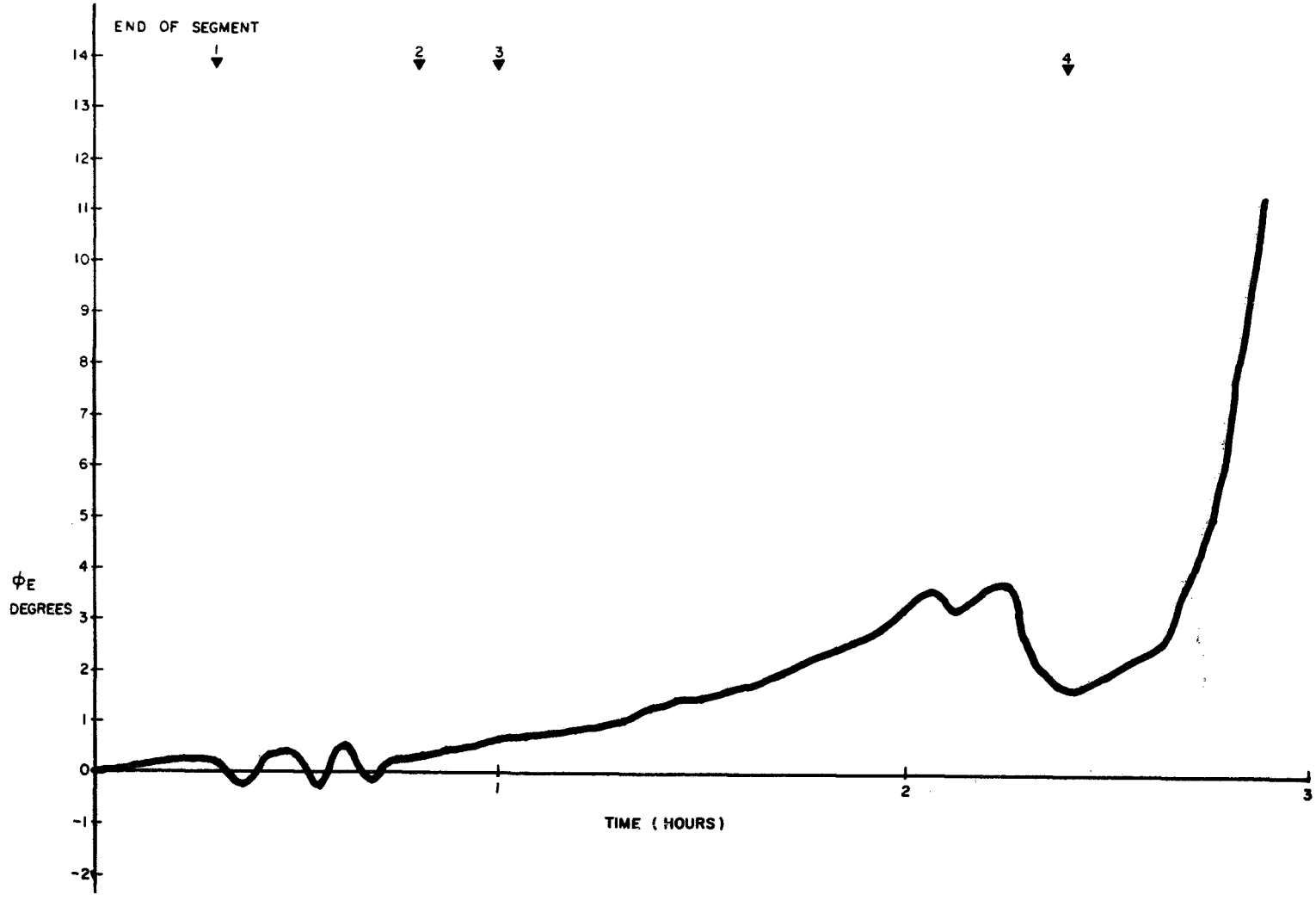

Figure 20. Bearing angle error for drift rates of A1 = -1, A2 = -1, A3 = -1, A4 = -1 deg/hour.

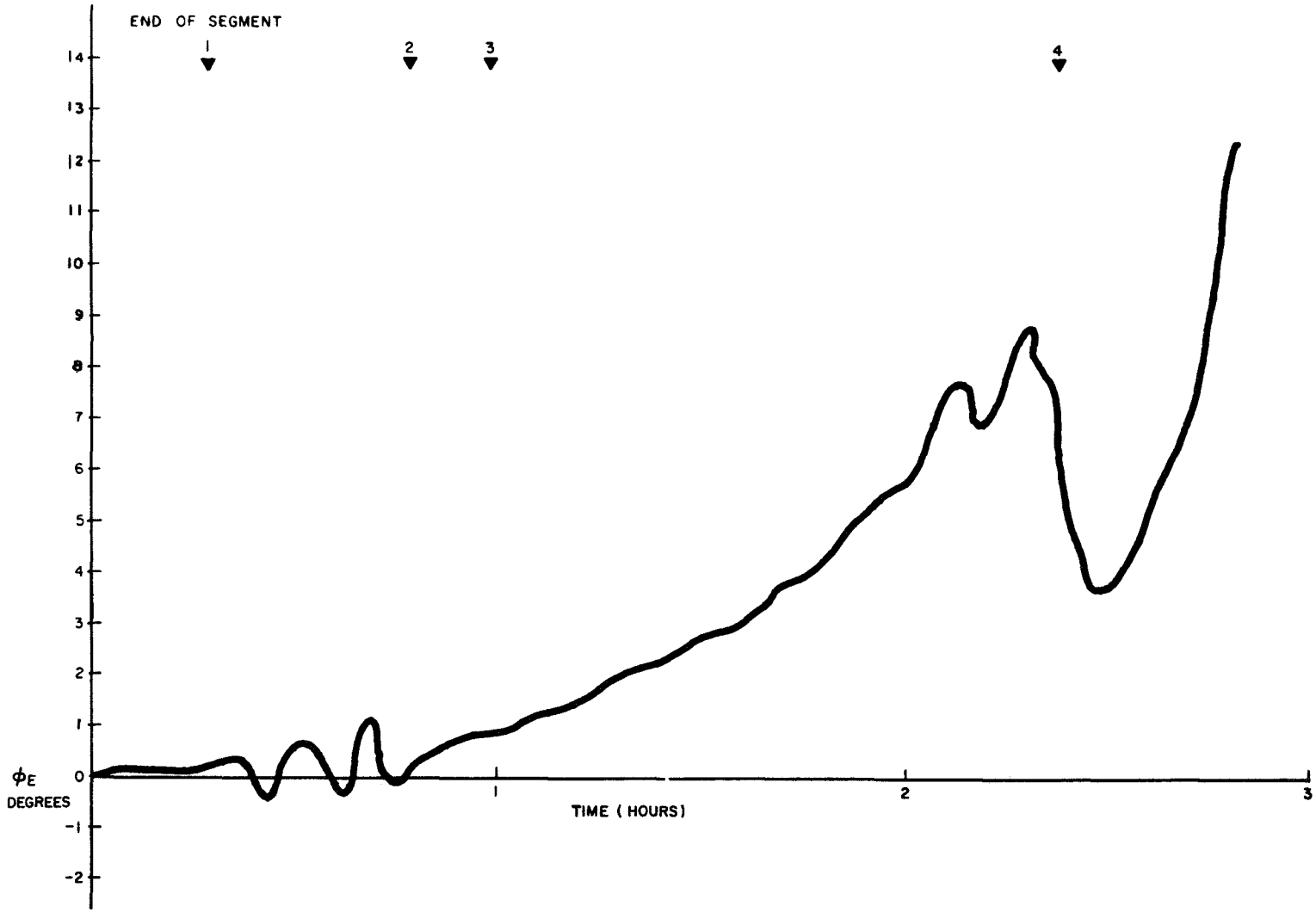

Figure 21. Bearing angle error for drift rates of A1 = -2, A2 = -2, A3 = -2, A4 = -2 deg/hour.

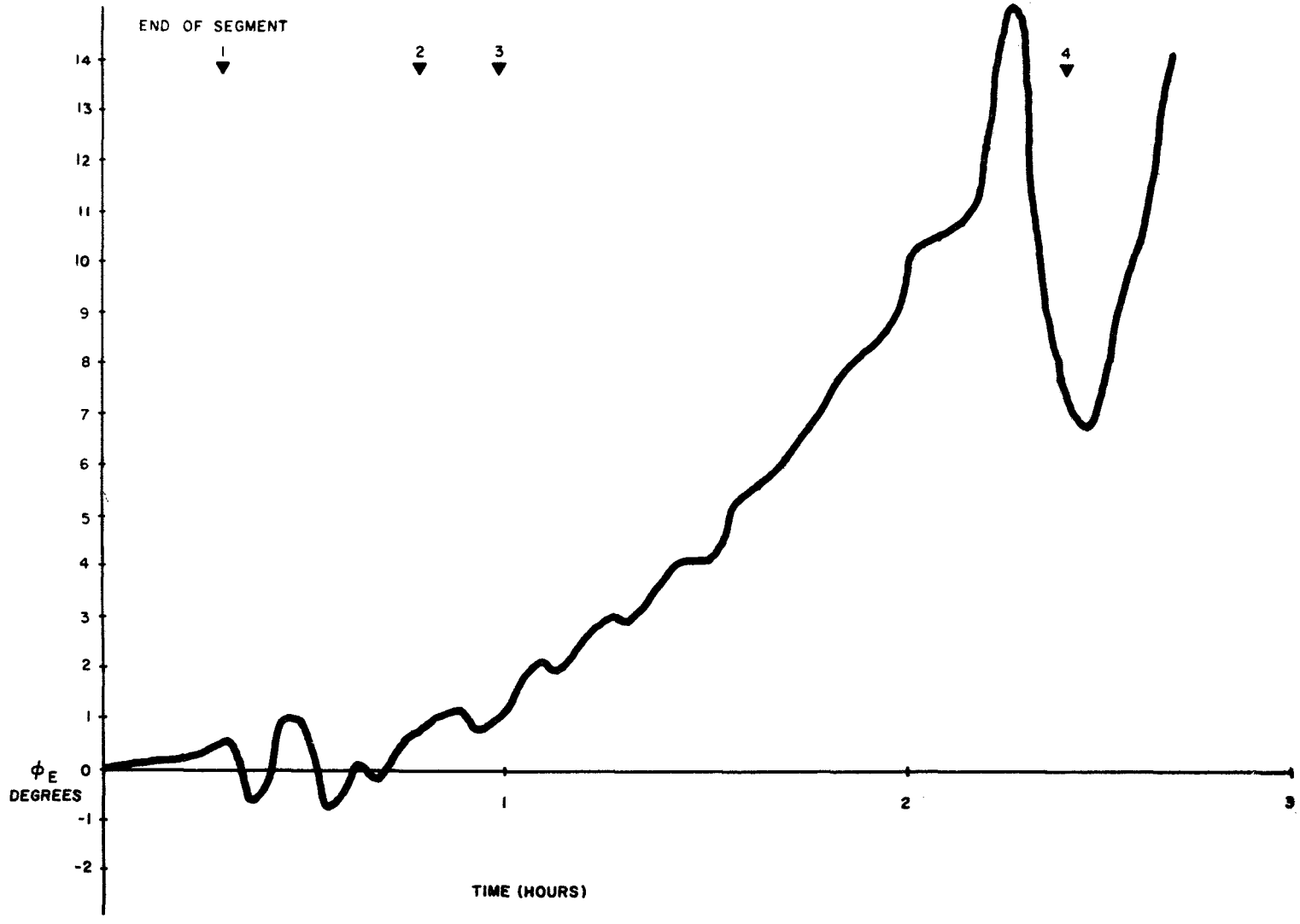

Figure 22. Bearing angle error for drift rates of A1 = -3, A2 = -3, A3 = -3, A4 = -3 deg/hour.

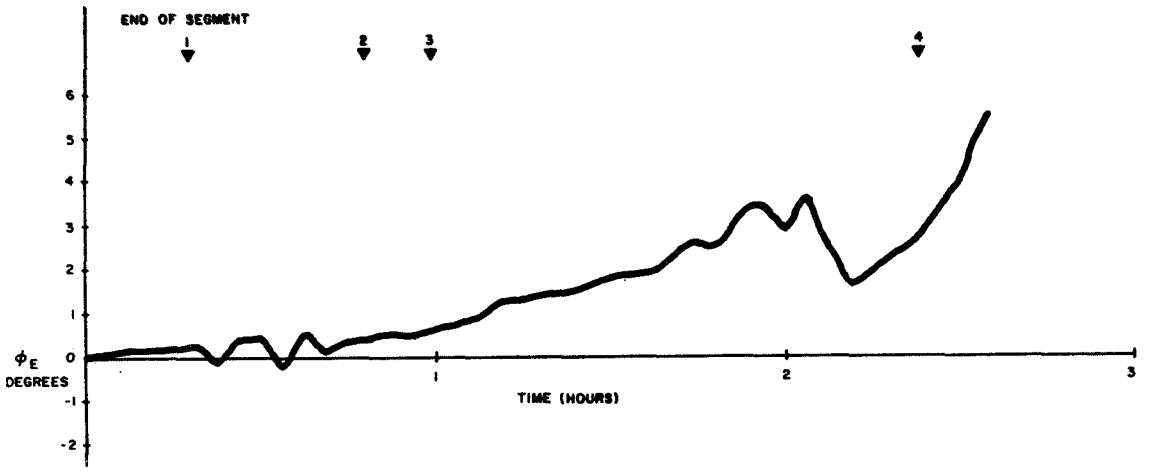

Figure 23. Bearing angle error for drift rates of A1 = +1, A2 = -1, A3 = +1, A4 = -1 deg/hour.

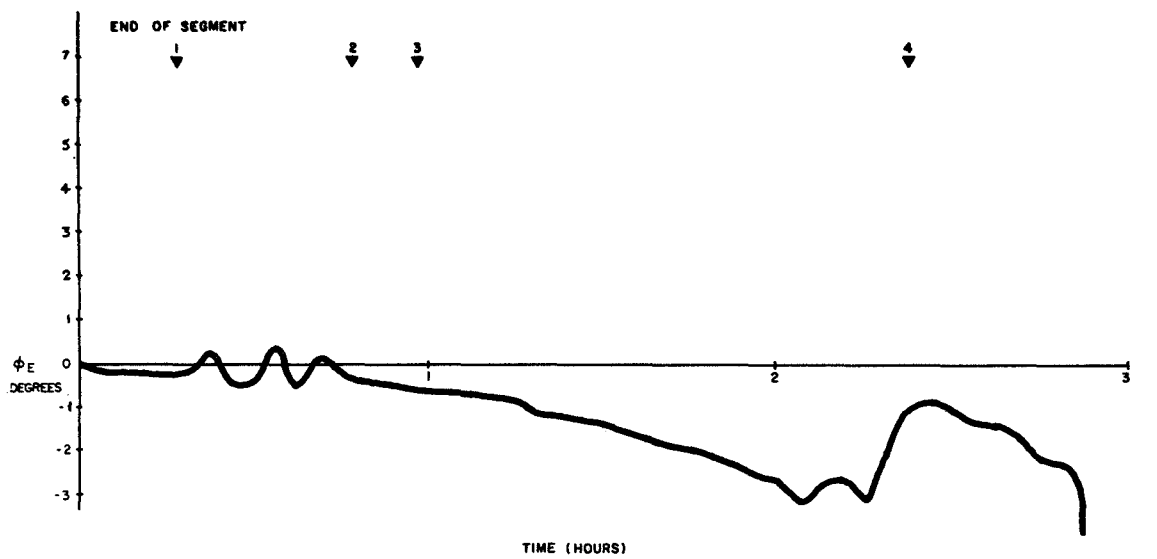

Figure 24. Bearing angle error for drift rates of A1 = -1, A2 = +1, A3 = -1, A4 = +1 deg/hour.

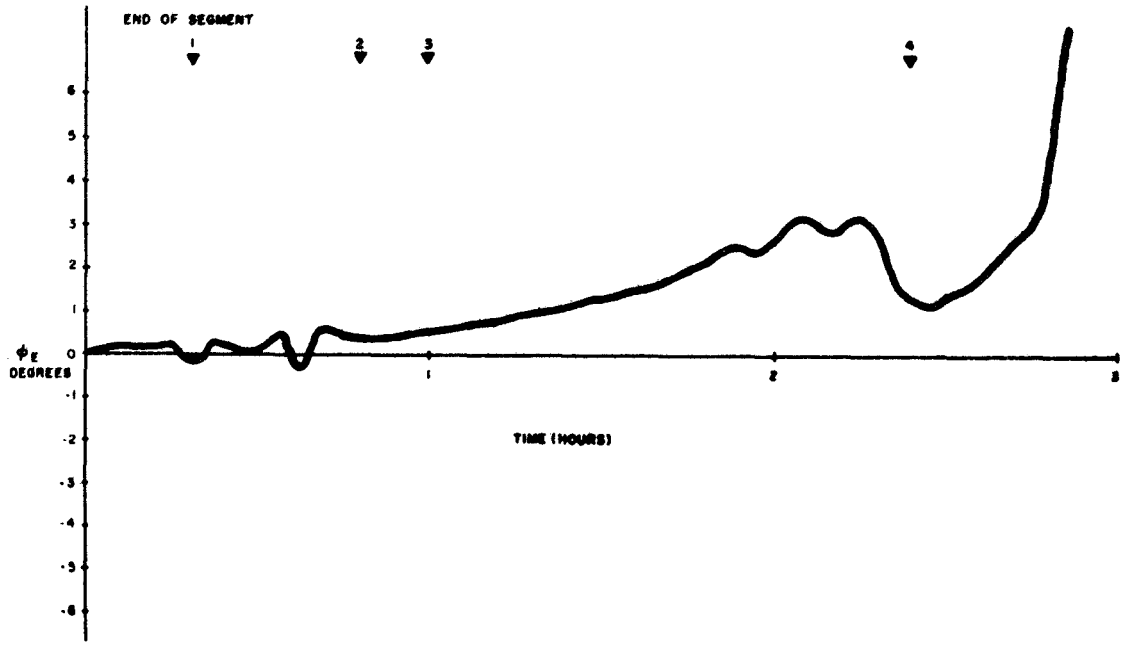

Figure 25. Bearing angle error for drift rates of A1 = -1, A2 = -1, A3 = +1, A4 = +1 deg/hour.

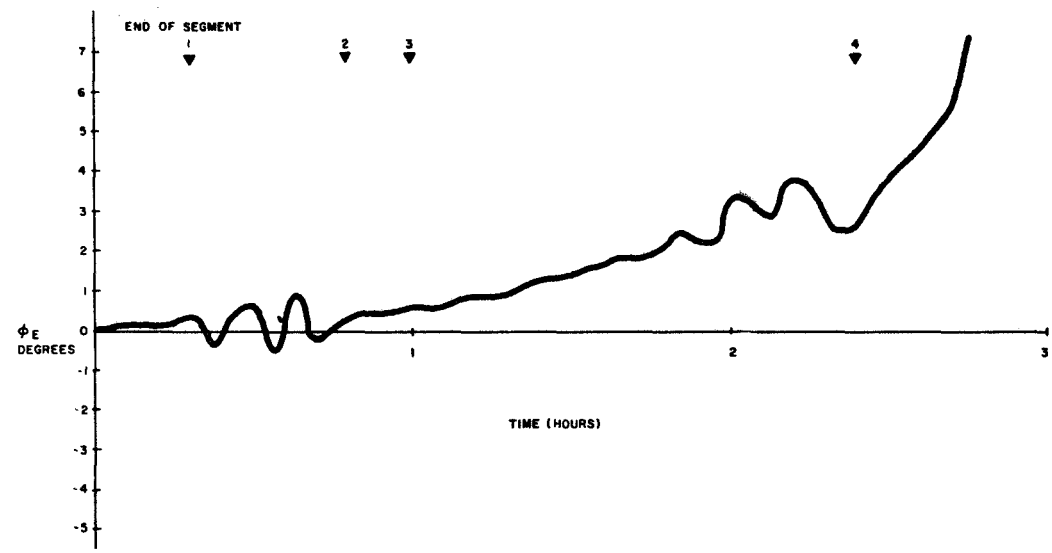

Figure 26. Bearing angle error for drift rates of A1 = +2, A2 = -1, A3 = +2, A4 = -2 deg/hour.

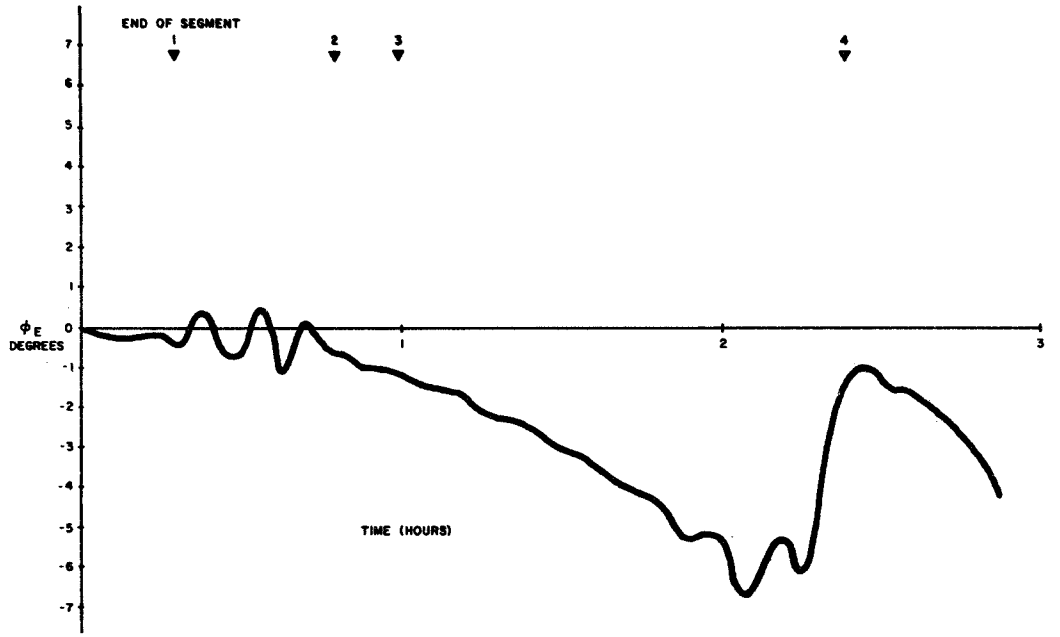

Figure 27. Bearing angle error for drift rates of A1 = -2, A2 = +2, A3 = -2, A4 = +2 deg/hour.

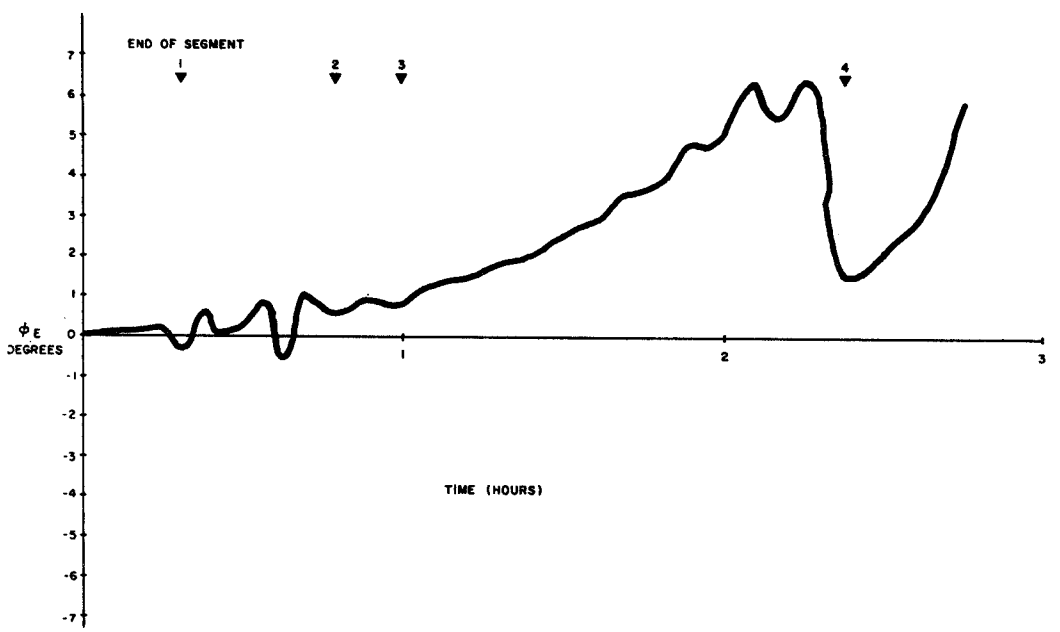

Figure 28. Bearing angle error for drift rates of A1 = -2, A2 = -2, A3 = +2, A4 = +2 deg/hour.

and give a bearing angle to the LEM of ϕ_B. The error in the bearing angle is defined as $\phi_E = \phi_A - \phi_B$. If the driver turns the vehicle through an angle ϕ_B with the vehicle located at point A, the error in the bearing angle is ϕ_E. The angle ϕ_E versus time is plotted in Figures 17 through 28. As the vehicle approaches the LEM site, the bearing angle error always increases in magnitude. The reason for this increase is easily understood by referring to Figure 29. When the range distance becomes small (less than 300 meters), ϕ_B can be considerably greater in magnitude than ϕ_A. Although the resulting error, ϕ_E, is large, it is not significant because the vehicle driver can easily observe the location of the LEM within the 300-meter range.

The second area of interest in the simulation study is the effects of vehicle misalignments. The ability to revisit an established site depends upon how well the vehicle can be realigned to the original reference direction. The effects of misalignments can easily be evaluated by intentionally offsetting the sequential angles A3, A4, and L. Cases 13 through 23 in Table 1 give the misalignments that were simulated. The misalignment errors were evaluated by the instantaneous radial error expressed by

$$\Delta R_T(t)_{t=t_a} = \sqrt{\left[X_I(t_a) - X_{IE}(t_a)\right]^2 + \left[Y_I(t_a) - Y_{IE}(t_a)\right]^2 + \left[Z_I(t_a) - Z_{IE}(t_a)\right]^2}$$

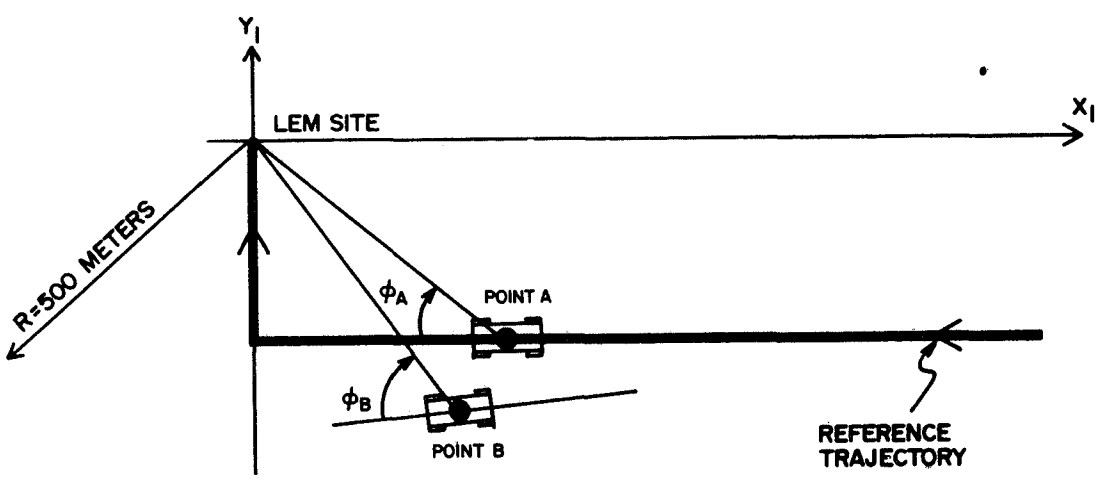

Figure 29. Heading angle error.

where $X_I(t_a)$, $Y_I(t_a)$, $Z_I(t_a)$ are the coordinates along the reference path at $t = t_a$, and $X_{IE}(t_a)$, $Y_{IE}(t_a)$, $Z_{IE}(t_a)$ are the coordinates at $t = t_a$ as given by the navigation system when misalignment errors are added. Figures 30 through 40 show the variations in ΔR_T as a function of time. ΔZ is the most significant component of ΔR_T and represents the vehicle altitude error. If altitude errors are neglected (this is reasonable since the vehicle must remain on the lunar surface), the important error is the in-plane error given by

$$\Delta R_{TP}(t)\Big|_{t=t_a} = \sqrt{\left[X_I(t_a) - X_{IE}(t_a)\right]^2 + \left[Y_I(t_a) - Y_{IE}(t_a)\right]^2}$$

This error, as a function of time, is illustrated in Figures 30 through 40.

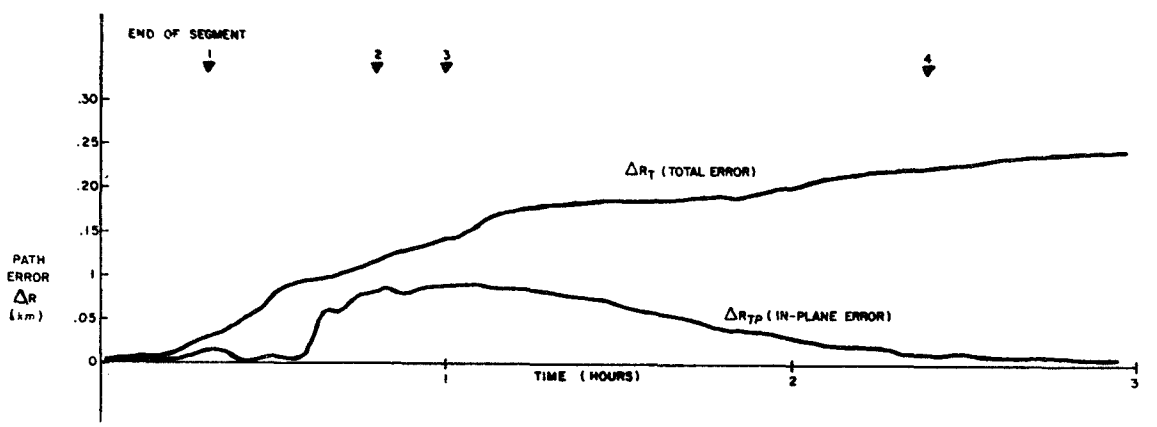

Figure 30. Radial path error versus time for vehicle misalignments of A3 = + 1 deg, A4 = +1 deg, L = +1 deg.

Nominal in-plane errors are noted from the diagrams to be generally less than 200 meters. The system requirement is that the vehicle must have navigation capability to revisit an established site. The ability to revisit a site depends upon land identification marks in the site area. Site identification can be established by flag markers or low level signal radio transmitters. In any case the navigation system must be capable of returning the vehicle to within identification range. A navigation system with a site return accuracy

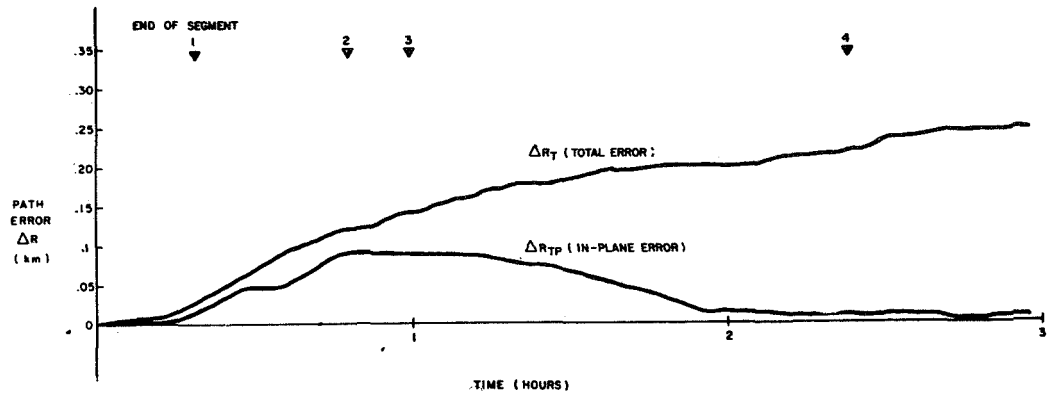

Figure 31. Radial path error versus time for vehicle misalignments of A3 = -1 deg, A4 = -1 deg, L = -1 deg.

of 200 to 300 meters should be adequate for relocating any given point within the maximum 5-km radial distance from the LEM. The preliminary simulation results indicate that misalignments should be less than 5 degrees to return to within 300 meters of any established site on the path profile.

CONCLUSIONS

The basic hardware required to implement the navigation scheme for lunar exploration is two free gyros mounted to the frame of the vehicle. A particular lunar trajectory was selected to evaluate the accuracy of the system. The time varying sequential angles were used as inputs for a digital simulation to study gyro drift rates and vehicle misalignments. The results of the simulation study indicate that system requirements can be satisfied with this navigation scheme. To meet the requirement of ±3 degrees pointing accuracy to the LEM site, the gyro drift rates should be in the range of 1 degree/hour. The capability to revisit any point (within 300 meters of accuracy) requires vehicle realignment accuracy of 5 degrees or less.

This navigation scheme represents only one of many possible candidates. Particular hardware configurations that should be analyzed include a directional and vertical gyro system, a sun aspect sensor and vertical gyro system, and a directional gyro and inclinometer system. The navigation equations for each

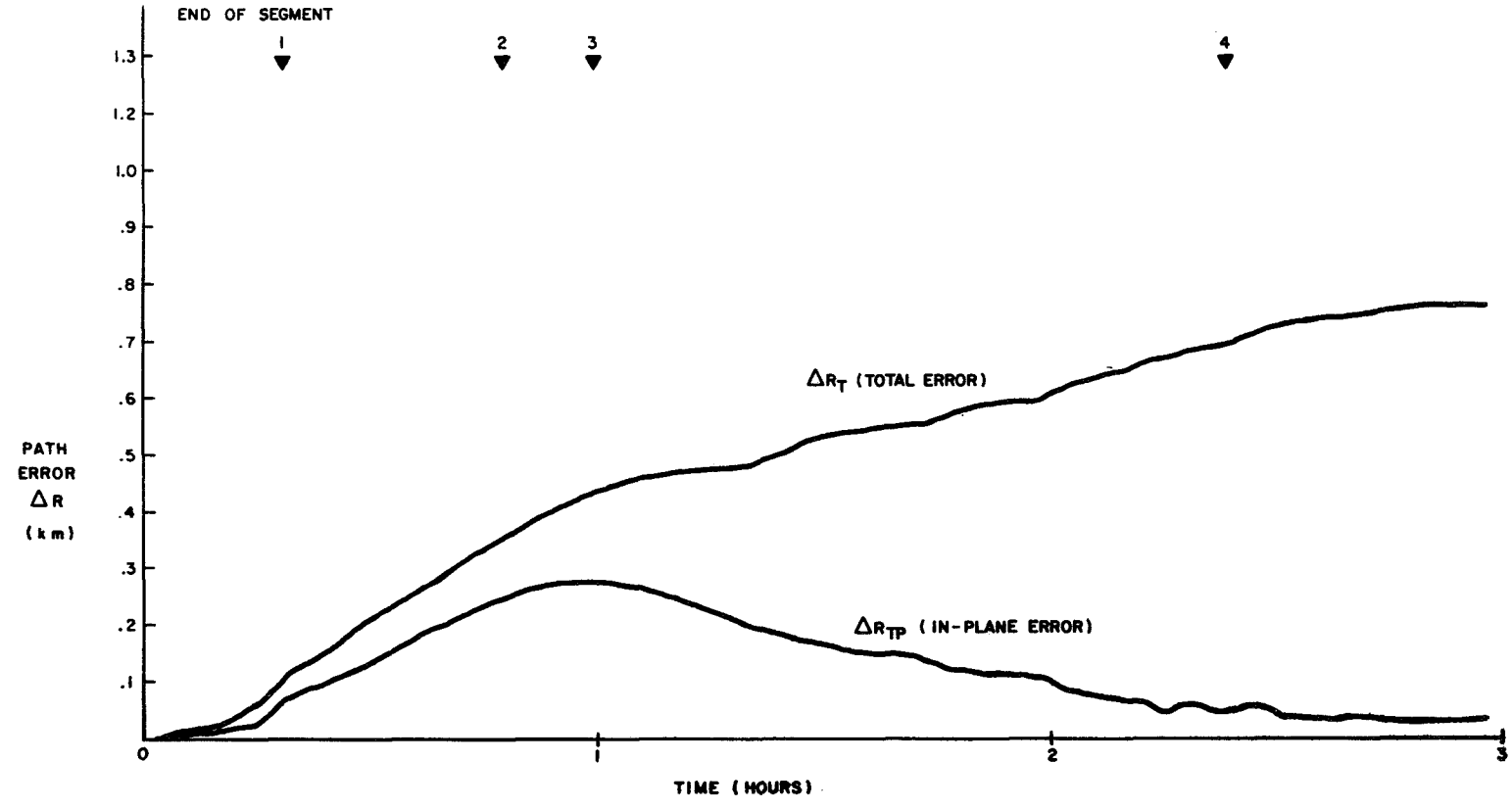

Figure 32. Radial path error versus time for vehicle misalignments of A3 = +3 deg, A4 = +3 deg, L = +3 deg.

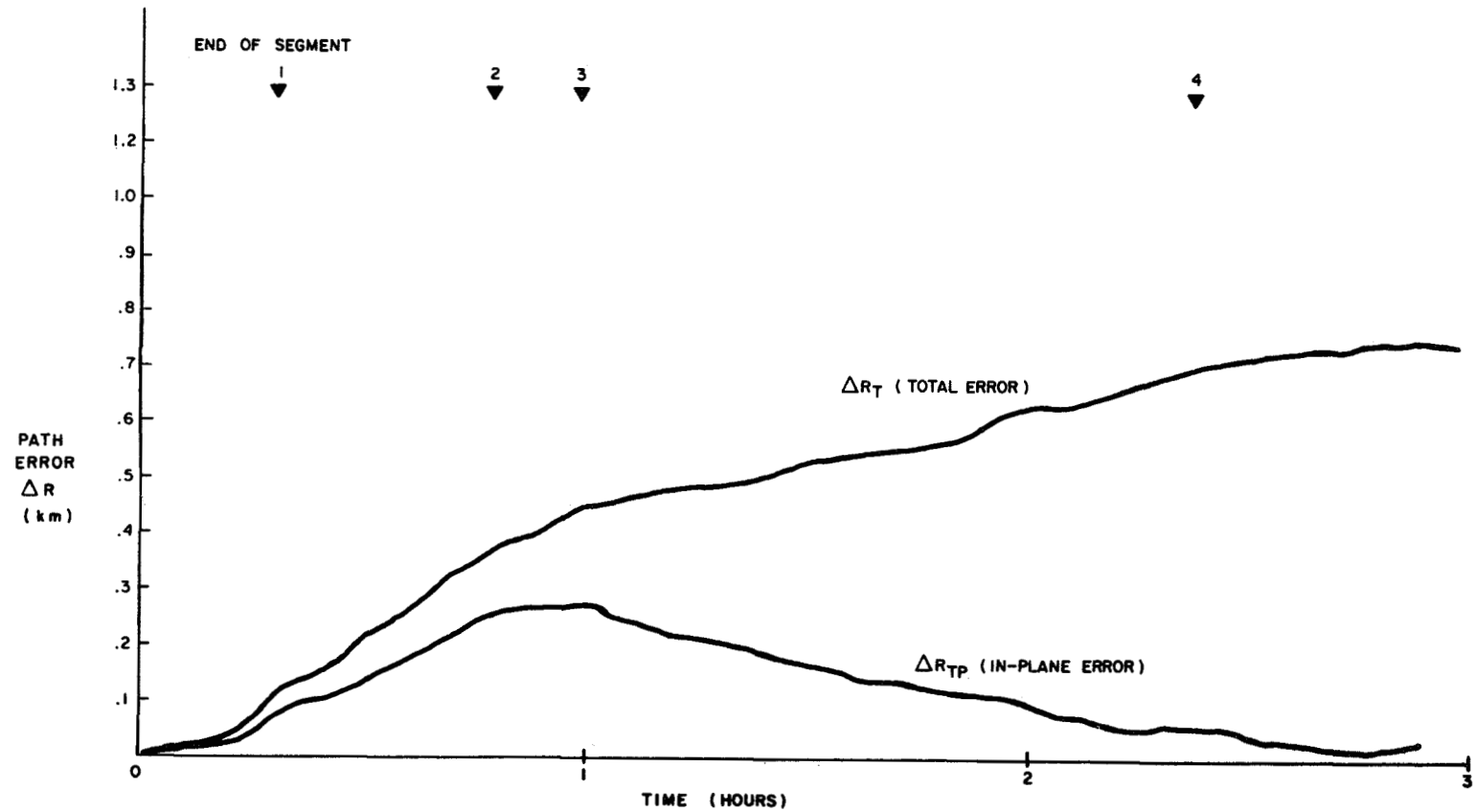

Figure 33. Radial path error versus time for vehicle misalignments of A3 = -3 deg, A4 = -3 deg, L = -3 deg.

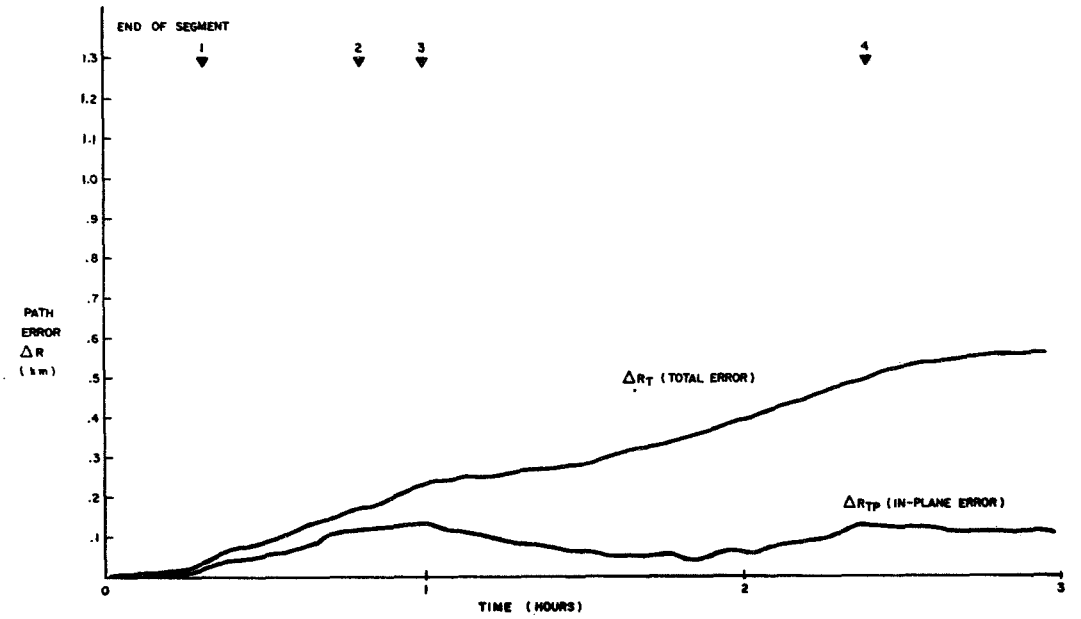

Figure 34. Radial path error versus time for vehicle misalignments of A3 = 1 deg, A4 = 1 deg, L = 1 deg and drift rates of 1 deg/hour.

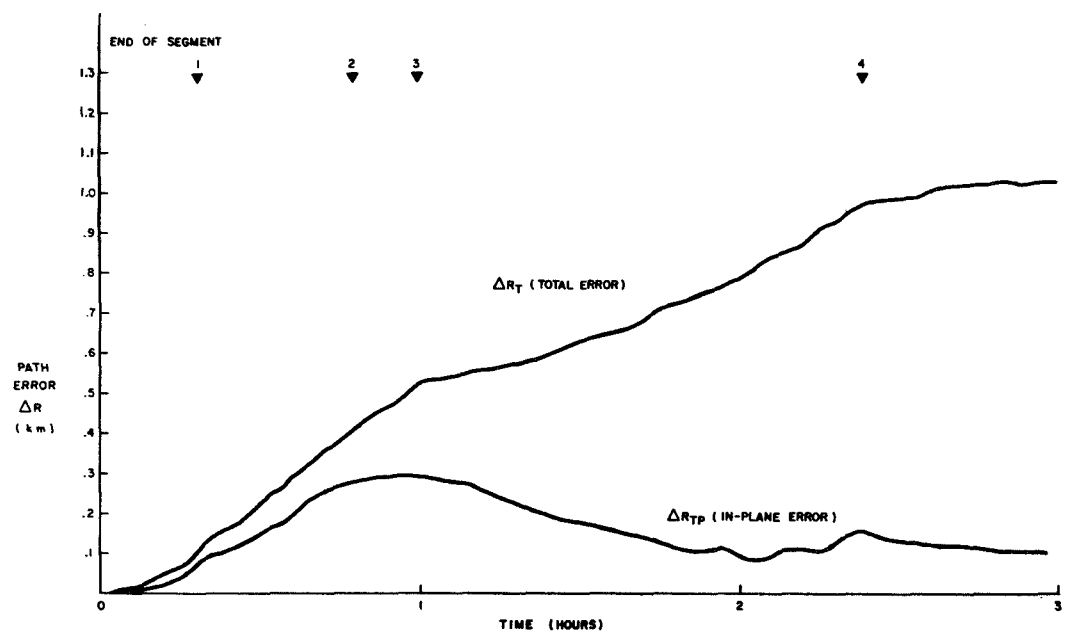

Figure 35. Radial path error versus time for vehicle misalignments of A3 = +3 deg, A4 = +3 deg, L = 3 deg and drift rates of +1 deg/hour.

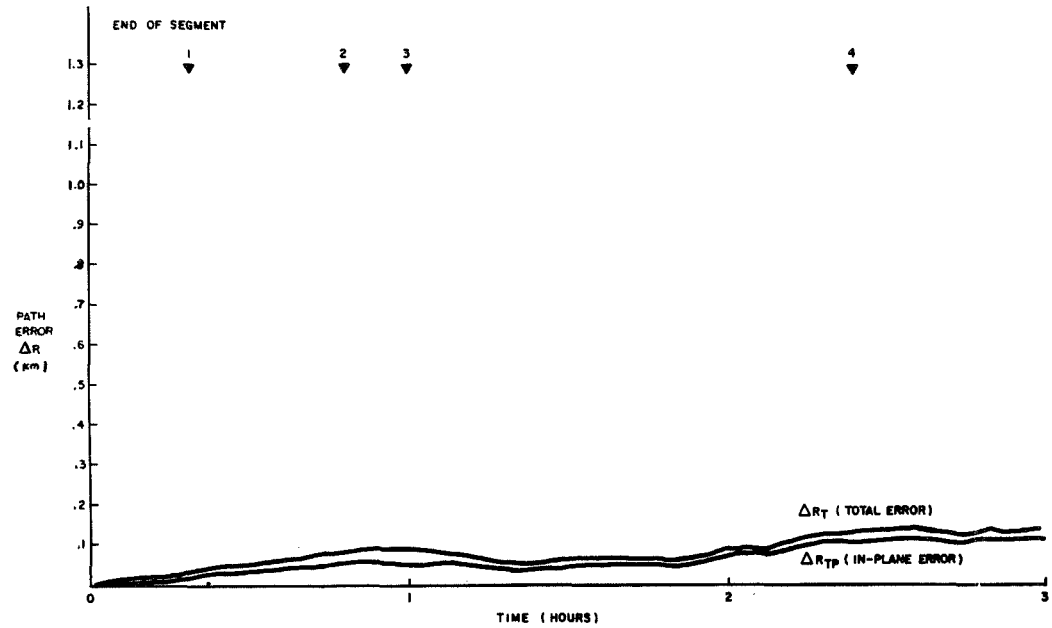

Figure 36. Radial path error versus time for vehicle misalignments of A3 = 1 deg, A4 = 1 deg, L = 1 deg and drift rates of -1 deg/hour.

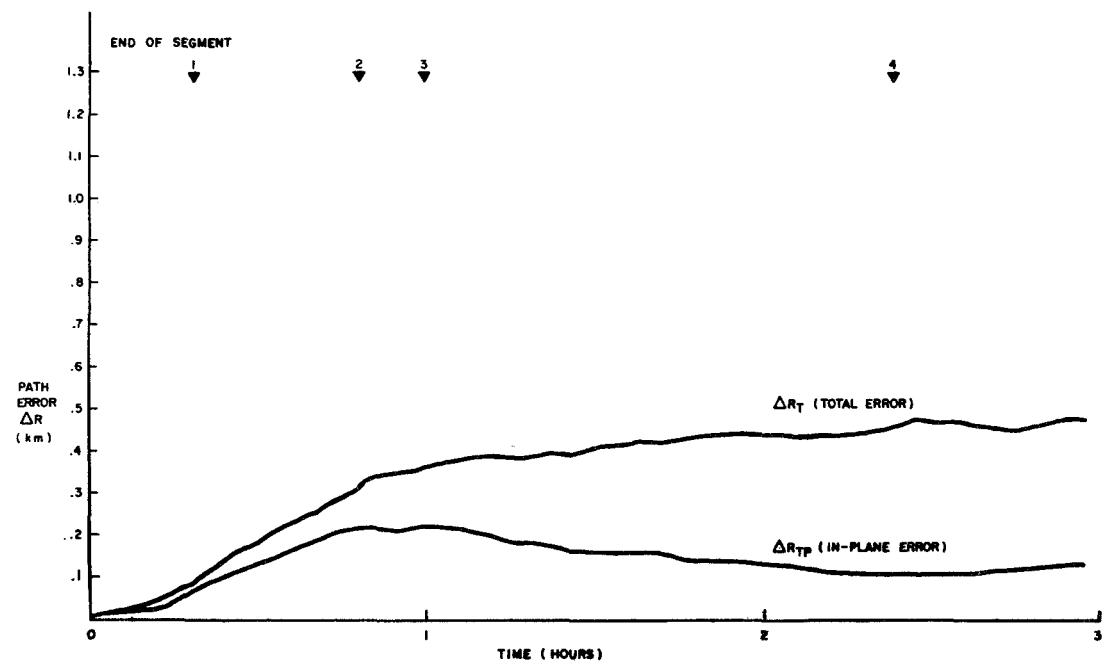

Figure 37. Radial path error versus time for vehicle misalignments of A3 = +3 deg, A4 = +3 deg, L = +3 deg and drift rates of -1 deg/hour.

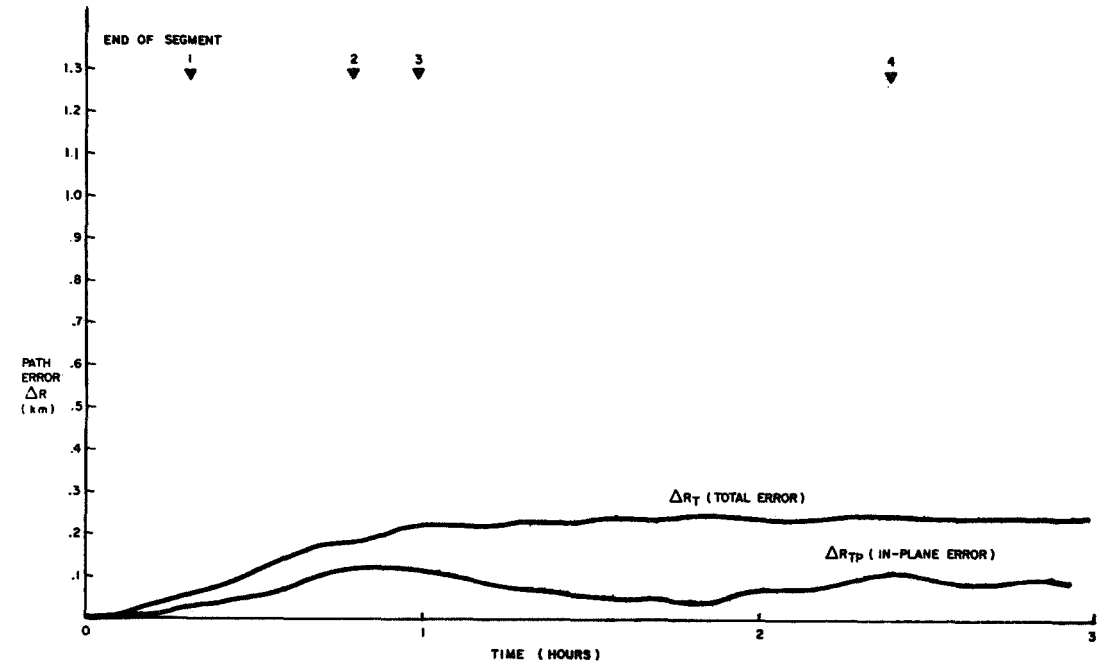

Figure 38. Radial path error versus time for vehicle misalignments of A3 = +1 deg, A4 = -2 deg, L = 3 deg and drift rates of +1 deg/hour.

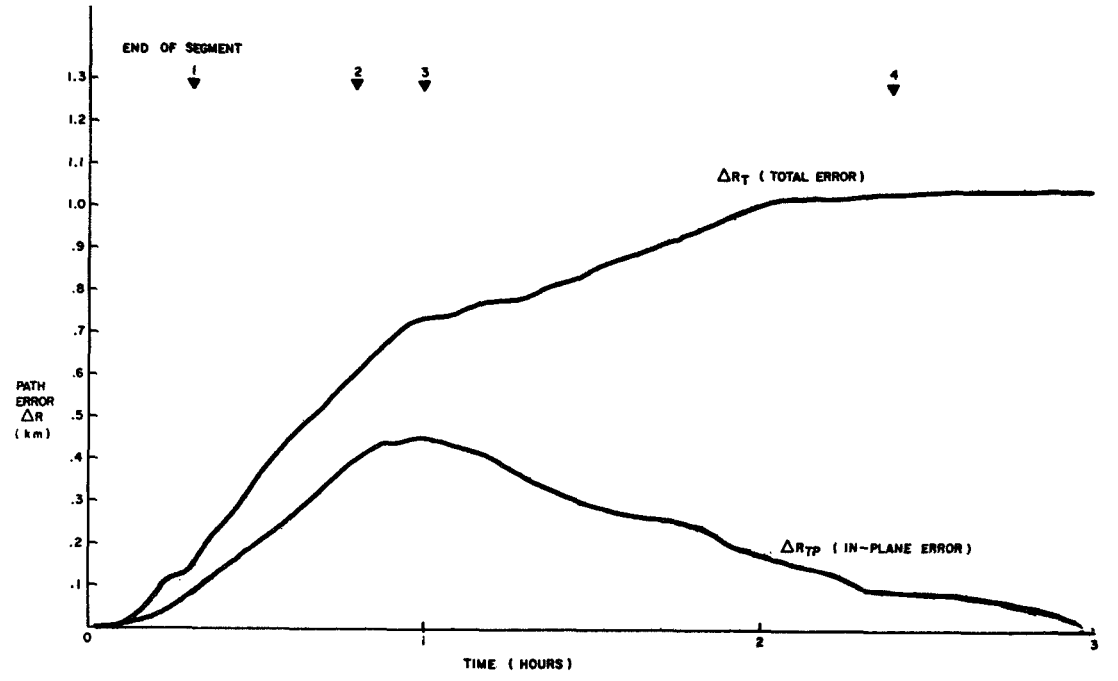

Figure 39. Radial path error versus time for vehicle misalignments of A3 = +5 deg, A4 = +5 deg, L = +1 deg.

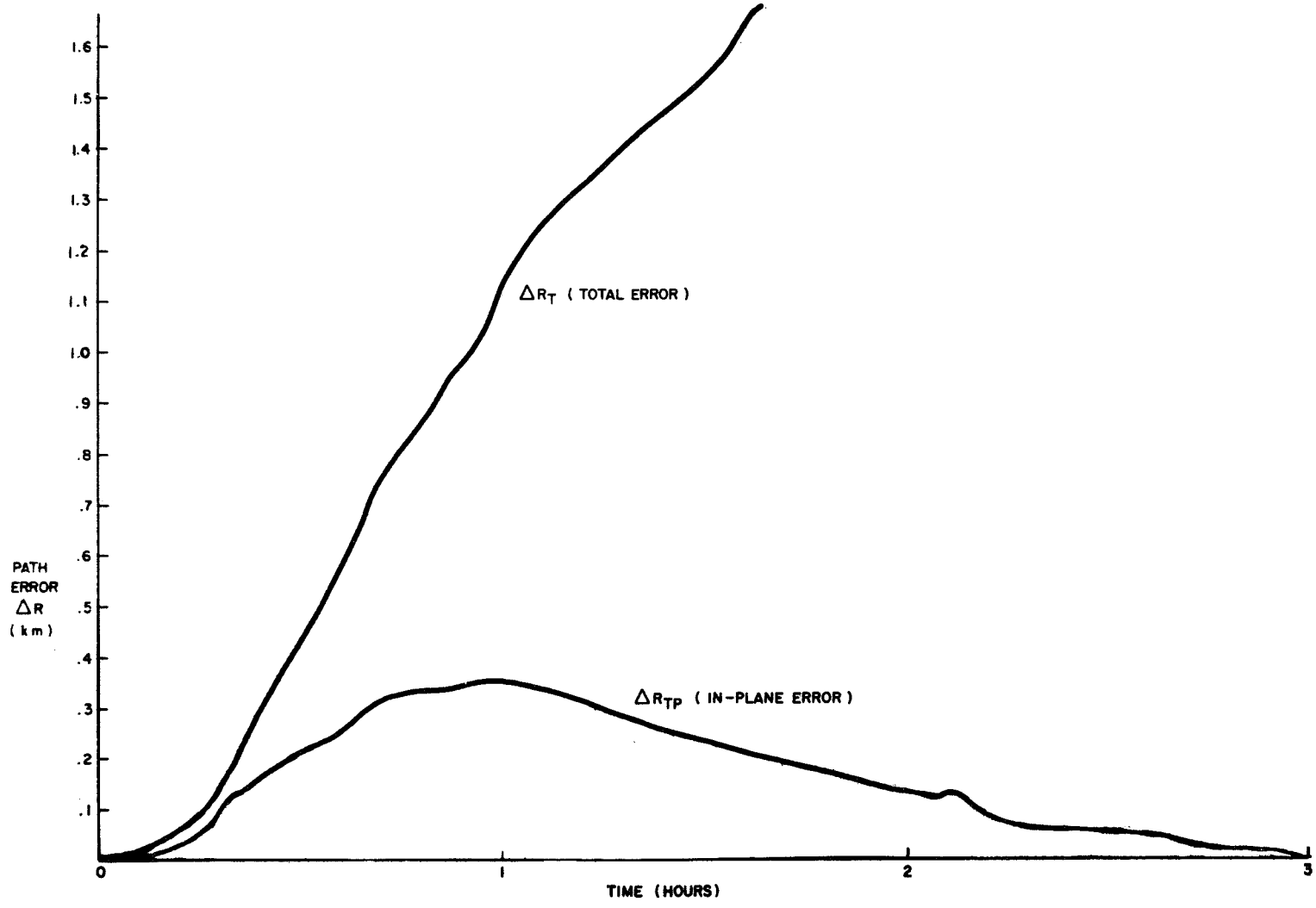

Figure 40. Radial path error versus time for vehicle misalignments of A3 = + 4 deg, A4 = +10 deg, L = 1 deg.

of these systems should be developed and related directly to measurable angles from the hardware. Simulation studies should be made to determine the system accuracy. Finally, a system selection should be made which represents the best compromise between cost, weight, reliability, minimum component development, and navigation accuracy.

APPENDIX

Figure A-1 gives the flow chart of the navigation system simulation. The program listing is given in Figure A-2.

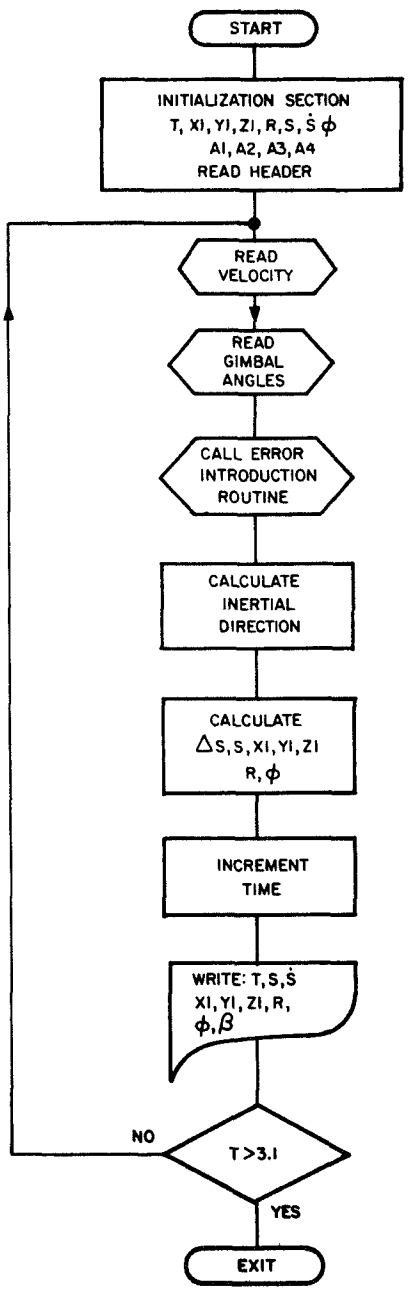

Figure A-1. Flow chart of navigation system simulation.

```
C       LUNAR ROVER VERSION TWO
        DIMENSION A(4),A1(4),A2(4)
        DATA T/0./
        DATA XI/0./
        DATA YI/0./
        DATA ZI/0./
        DATA DELTA/.00390625/
        DATA S/0./
        DATA R/0./
        DATA V1,V2/0.,0./
        DATA FEE/0./
C       ODOMETER
C        BEARING AND INCLINATION
        CALL HEADNG
        WRITE(5,1) T,S,V2,ZI,XI,YI,R,FEE,B
        CALL VELOC(T,V1)
    2   CALL VELOC((T+DELTA),V2)
        CALL GIMBAL(T,A)
        CALL ERROR (T,A)
        CALL BEARNG(A,B)
        DS=((V1+V2)/2.)*DELTA
        S=S+DS
C       COORDINATE DISPLACEMENTS
        ZI=ZI+DS*SIN(A(3))
        HD=DS*COS(A(3))
        XI=XI+HD*COS(B)
        YI=YI+HD*SIN(B)
C       RANGE
        R=SQRT(XI*XI+YI*YI+ZI*ZI)
C       DIRECTION TO HOME BASE
        CALL ANGLE(YI,XI,THETA)
        FEE=3.141592653589793+THETA-B
        T=T+DELTA
C       OUTPUT TO GUAGES
        WRITE(5,1) T,S,V2,ZI,XI,YI,R,FEE,B
        IF(T.GT.3.10) CALL EXIT
        V1=V2
        DO 6 K=1,4,1
    6   A1(K)=A2(K)
        GO TO 2
    1   FORMAT(9(F12.8,2X))
        END
```

Figure A-2. Simulation program listing.

```
      SUBROUTINE VELOC(T,V)
      DIMENSION TR(5)
      DATA TR(1),TR(2),TR(3),TR(4),TR(5)/.3,.792,.994,2.39,3.0/
      IF(T.LE.TR(1)) GO TO 1
      IF(T.LE.TR(2)) GO TO 2
      IF(T.LE.TR(3)) GO TO 3
      IF(T.LE.TR(4)) GO TO 4
      IF(T.LE.TR(5)) GO TO 5
      V=0.
      RETURN
    1 V=30.*T
      RETURN
    2 V=9.0
      RETURN
    3 V=9.0
      RETURN
    4 V=4.60983
      RETURN
    5 V=1.8851
      RETURN
      END


      SUBROUTINE ERROR(T,A)
      DIMENSION A(4)
      RETURN
      END


      SUBROUTINE GIMBAL(T,A)
      DIMENSION A(4)
      CALL DRIVER(T,A,AL)
      SA1=(SIN(A(4))*SIN(AL)+COS(A(4))*SIN(A(3))*COS(AL))
      CA1=SQRT(1.-SA1*SA1)
      CALL ANGLE(SA1,CA1,A(1))
      SA2=COS(A(4))*SIN(AL)-SIN(A(4))*SIN(A(3))*COS(AL)
      CA2=COS(A(3))*COS(AL)
      CALL ANGLE(SA2,CA2,A(2))
      RETURN
      END
```

Figure A-2. (Continued)

```
      SUBROUTINE DRIVER(T,A,AL)
      DIMENSION TR(5),A(4)
      DATA TR(1),TR(2),TR(3),TR(4),TR(5)/.3,.792,.994,2.39,3.0/
      DATA FAC/0.017453292519943/
      DATA PI/3.141592653589793/
      DATA W2/38.2085592993/
      DATA W3/314.1592653589793/
      IF(T.LE.TR(1)) GO TO 1
      IF(T.LE.TR(2)) GO TO 2
      IF(T.LE.TR(3)) GO TO 3
      IF(T.LE.TR(4)) GO TO 4
      IF(T.LE.TR(5)) GO TO 5
      RETURN
    1 AL=.5235988
      A(3)=0.
      A(4)=0.
      RETURN
    2 AL=0.
      A(4)=0.
      A(3)=FAC*46.29*COS(W2*(T-TR(1)))
      RETURN
    3 AL=-1.5707963
      A(3)=0.
      A(4)=.5235988*SIN(W3*(T-TR(2)))
      RETURN
    4 AL=PI-57.4*FAC*COS(31.5059435164*      (T-TR(4)))
      A(3)=0.
      A(4)=0.
      RETURN
    5 AL=1.5707963
      A(3)=0.
      A(4)=0.
      RETURN
      END
```

Figure A-2. (Continued)

```
      SUBROUTINE BEARNG(A,B)
      DIMENSION A(4)
      SB=COS(A(1))*SIN(A(2))*COS(A(4))+SIN(A(1))*SIN(A(4))
      CB=COS(A(1))*COS(A(2))*COS(A(3))-COS(A(1))*SIN(A(2))*SIN(A(4))*SIN(A(3))
     1(A(3))+SIN(A(1))*COS(A(4))*SIN(A(3))
      CALL ANGLE(SB,CB,B)
      RETURN
      END


      SUBROUTINE ANGLE(SB,CB,B)
      B=ATAN2(SB,CB)
      RETURN
      END
      SUBROUTINE HEADNG
      WRITE(5,1)
    1 FORMAT(1H1,40X,'LUNAR ROVER VERSION TWO'//20X,'ALL DISTANCES IN KM'/20X,'A
     1'/20X,'ALL ANGLES IN RADIANS'/20X,'TIME IN HOURS'//'T',13X,'S',13X,
     1,'V',13X,'ZI',12X,'XI',12X,'YI',12X,'R',13X,'FEE',11X,'BETA')
      RETURN
      END
```

Figure A-2. (Concluded)

REFERENCES

1. Lunar Navigation Study Final Report (Summary Volume). BSR 1134, Contract No. NAS8-11292, The Bendix Corporation, Bendix Aerospace Systems Division, June 1965.

2. Lunar Navigation Study Final Report (Sections 1 through 7). BSR 1134, Contract No. NAS8-11292, The Bendix Corporation, Bendix Aerospace Systems Division, June 1965.

3. Mobile Geological Laboratory Navigation System Description. BSR 1243, Contract No. NAS8-20273, The Bendix Corporation, Bendix Aerospace Systems Division, February 1966.

4. Conceptual Design for Mobile Geological Laboratory Position and Heading Fix System. BSR 1257, The Bendix Corporation, Bendix Aerospace Systems Division, March 1966.

5. Lunar Navigation Study Final Report (Volume I). BSR 1472, Contract No. NAS8-20322, The Bendix Corporation, Bendix Aerospace Systems Division, December 1966.

6. LSSM for Apollo Applications Program. Final Report, Volume II, Book 8, Appendix G, Navigation Analysis. BSR 1495, Contract No. NAS8-20378, The Bendix Corporation, Bendix Systems Division, February 1967.

APPROVAL

A SIMPLIFIED DEAD RECKONING NAVIGATION SYSTEM FOR THE MANNED LUNAR ROVING VEHICLE

By Walter L. Green

The information in this report has been reviewed for security classification. Review of any information concerning Department of Defense or Atomic Energy Commission programs has been made by the MSFC Security Classification Officer. This report, in its entirety, has been determined to be unclassified.

This document has also been reviewed and approved for technical accuracy.

Melvin Brooks

MELVIN BROOKS
Chief, Guidance and Control Systems Branch

F. S. Wojtalik

F. S. WOJTALIK
Chief, Systems Division

F. B. Moore

F. B. MOORE
Director, Astrionics Laboratory

DIR
Dr. von Braun

S&E-DIR
Dr. McDonough

S&E-CSE-DIR
Dr. Haeussermann
Mr. Mack

S&E-CSE-I
Mr. Hammers
Mr. Blackstone

S&E-CSE-M
Mr. Haygood

S&E-AERO-DIR
Dr. Geissler
Mr. Horn

S&E-AERO-DOD
Mr. Worley

S&E-ASTR-DIR
Mr. Moore

S&E-ASTR-A
Mr. Hosenthien
Dr. Seltzer
Dr. Nurre
Dr. Borelli
Mr. Clark
Mr. von Pragenau
Miss Flowers

S&E-ASTR-C
Mr. Swearingen
Mr. Fernandez
Mr. Hall

S&E-ASTR-G
Mr. Mandel
Dr. Doane
Mr. Doran
Mr. Jones
Mr. Broussard
Mr. Wood
Mr. Kalange
Mr. Walls

S&E-ASTR-I
Mr. Duggan

S&E-ASTR-M
Mr. Boehm
Mr. Thornton

S&E-ASTR-R
Mr. Taylor
Dr. Randall

S&E-ASTR-S
Mr. Wojtalik
Mr. Brandner
Mr. Gilino
Mr. Riley
Mr. Stroud
Mr. Cox
Mr. Brooks (10)
Mr. Scofield
Mr. Chubb
Mr. Neudatschin
Mr. Thompson
Mr. Smith
Mr. Blanton
Mr. Davis
Dr. Green (25)

S&E-ASTR-E
Mr. Aden

S&E-ASTR-ZX

A&TS-MS-IL (8)

A&TS-MS-IP (2)

A&TS-MS-H

A&TS-PAT
Mr. Wofford

A&TS-TU (15)
Mr. Winslow

PM-PR-M

DEP-T

AD-S

Scientific and Technical Information Facility (2)
P. O. Box 33
College Park, Maryland 20740
Attn: NASA Representative (S-AK/RKT)